Distributed H_∞ Controller Design and Robustness Analysis for Vehicle Platooning Under Random Packet Drop

Kaushik Halder, Umberto Montanaro, Shilp Dixit, Mehrdad Dianati, *Senior Member, IEEE*, Alexandros Mouzakitis, and Saber Fallah

***Abstract*— This paper presents the design of a robust distributed state-feedback controller in the discrete-time domain for homogeneous vehicle platoons with undirected topologies, whose dynamics are subjected to external disturbances and under random single packet drop scenario. A linear matrix inequality (LMI) approach is used for devising the control gains such that a bounded H_∞ norm is guaranteed. Furthermore, a lower bound of the robustness measure, denoted as γ gain, is derived analytically for two platoon communication topologies, i.e., the bidirectional predecessor following (BPF) and the bidirectional predecessor leader following (BPLF). It is shown that the γ gain is highly affected by the communication topology and drastically reduces when the information of the leader is sent to all followers. Finally, numerical results demonstrate the ability of the proposed methodology to impose the platoon control objective for the BPF and BPLF topology under random single packet drop.**

***Index Terms*— Vehicle platoon, LMI, distributed H_∞ control with packet drops, robustness of closed-loop system.**

I. Introduction

A PLATOON of vehicles is a group of two or more consecutive connected autonomous vehicles (CAVs) which travel at the same speed with a short inter-vehicular distance. The first vehicle in the fleet also known as platoon leader, usually dictates the platoon speed, which is then imposed to the other vehicles in the string, denoted as followers, through control systems. The organisation of CAVs in platoons offers several benefits in highway driving scenarios such as road safety, highway utility and fuel economy [1], [2].

Manuscript received February 10, 2020; revised September 3, 2020 and November 16, 2020; accepted November 23, 2020. Date of publication December 29, 2020; date of current version May 3, 2022. This work was supported in part by Jaguar Land Rover and in part by the Engineering and Physical Sciences Research Council (EPSRC), U.K., as part of the jointly funded "Towards Autonomy: Smart and Connected Control (TASCC) Programme," under Grant EP/N01300X/1. The Associate Editor for this article was J. E. Naranjo. *(Corresponding author: Saber Fallah.)*

Kaushik Halder, Shilp Dixit, and Saber Fallah are with the CAV-Lab, Department of Mechanical Engineering Sciences, University of Surrey, Guildford GU2 7XH, U.K. (e-mail: k.halder@surrey.ac.uk; s.dixit@surrey.ac.uk; s.fallah@surrey.ac.uk).

Umberto Montanaro is with the Department of Mechanical Engineering Sciences, University of Surrey, Guildford GU2 7XH, U.K. (e-mail: u.montanaro@surrey.ac.uk).

Mehrdad Dianati is with the Warwick Manufacturing Group (WMG), International Manufacturing Centre, University of Warwick, Coventry CV4 7AL, U.K. (e-mail: m.dianati@warwick.ac.uk).

Alexandros Mouzakitis is with Jaguar Land Rover Ltd., Coventry CV3 4LF, U.K. (e-mail: amouzak1@jaguarlandrover.com).

Digital Object Identifier 10.1109/TITS.2020.3044221

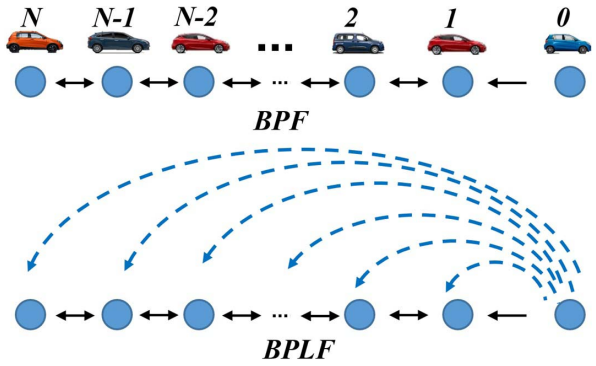

Fig. 1. Examples of undirected topologies for vehicle platooning: (a) the BPF topology and (b) the BPLF topology.

A platoon of vehicles can be either homogeneous or heterogeneous depending on the dynamics of the platoon vehicles. The platoon is said homogenous when the platoon vehicles have identical dynamics, otherwise, the vehicle platoon is called heterogeneous [3], [4]. To maintain the cooperative motion of vehicles in a platoon, the vehicles exchange their information with the neighbours using wireless communication systems like vehicle-to-vehicle (V2V) [5], [6] and vehicle-to-infrastructure (V2I) [6]. The pattern in which vehicles are connected in the platoon via wireless communications defines the network topology [1], [2]. A network topology can be either directed or undirected. The topology is said undirected when the communication for all the pairs of connected platoon followers is bidirectional, otherwise it is said directed [4], [7]. Typical topologies used to impose the platoon control objectives are the predecessor following (PF), the predecessor leader following (PLF), the bidirectional PF (BPF) [8], the bidirectional PLF (BPLF) and the all-to-all topology [9]. For example, PF topology represents unidirectional information exchange, where each vehicle in a platoon receives the information only from its immediate predecessor vehicle and sends its information only to the first follower vehicle. PF topology is a typical example of directed topology [4], [10]. In the BPF topology, each platoon vehicle exchanges information (i.e., sends and receives information) with its immediate predecessor and follower vehicle as shown in Fig. 1. The BPF topology is a typical example of undirected topology [10].

A detailed study of various information topologies for vehicle platoon has been reported in [10] and the references therein. However, the wireless communication network used for vehicle platooning could be effected by packet drops and/or communication delay in data transmissions among the vehicles as its reliability highly depends on bandwidth allocation, signal strength, external disturbances etc. Stability and control performance of vehicle platoon systems is affected by packet drops and/or communication delay and these communication constraints may also lead the vehicle platoon systems towards instability [11], [12]. Hence, the control challenge is to ensure the stability and the cooperative platoon motion with no ideal network system. To this aim, network imperfections should be systematically considered in the control design [13], [14].

In this paper, the longitudinal dynamics of homogeneous platoons are controlled. The proposed control desing ensures the internal stability and robust performance against random single packet drop and external disturbances acting on the dynamics of each platoon follower. To achieve this, the platoon control problem is first converted into a synchronisation problem of multi-agent systems as in [9], [14], [15] but affected by random packet drops modelled as a Bernoulli distribution and external disturbances. Then an LMI-based control design is used to compute the gains of the distributed controller to guarantee stability and robustness. Similar to [15], the resulting high dimensional LMI can be scaled to a single vehicle by considering the eigenvalues of the Laplacian and the pinning matrix associated to the platoon topology, thus facilitating its numerical solution. Finally, an analysis of the robustness measure is systematically carried out for two undirected platoon topologies, i.e., the BPF and BPLF topology.

The remainder of the paper is organized as follows. Section. II provides the related work for vehicle platooning and points out the contribution of the paper with respect to the current literature. Section. III describes the platoon modeling and the platoon control objectives as a synchronisation problem under random single packet drop scenario. The LMI-based distributed controller design approach to impose the platoon control objectives is presented in Section. IV while Section. V describes the robustness analysis of the vehicle platoon under single packet drop. Numerical results illustrating the effect of BPF and BPLF network topologies (with random single packet drop) on the H_∞ norm bound γ as a function of number of platoon members together with time-based simulation analysis are presented in Section. VI. Conclusions are drawn in Section. VII. Finally, the Appendix collects the systematic proofs of Theorems and Corollaries presented in the paper.

II. Related Works and Contribution of the Paper

The importance of network topology for the platoon problem have been recently pointed out by many researchers [4], [8], [9]. For example, Zheng *et al.* [4] designed a distributed controller and studied the impact of information flow topology on internal stability and scalability for homogeneous vehicle platoon using algebraic graph theory and the Routh-Hurwitz criteria. A distributed model predictive control was proposed for heterogeneous vehicle platoon system with directed topologies in [16]. To improve stability margin to homogeneous vehicle platoon systems with undirected topology, Zheng *et al.* [10] proposed to enlarge the information flow topology and considered asymmetric control strategy. An adaptive control strategy has been recently adopted in [9] for adjusting both the network topology and control gains of the distributed controllers based on the state mismatches among platoon vehicles where the use of the σ-modification strategy limits the growth of the adaptive gains in presence of external disturbances. By utilising adaptive topologies, it is possible to reduce the number of connections in the topology, thus reducing the network load and the risk of network congestion, while maintaining the cooperative platoon motion. Moreover, the adaptive control gains together with the σ-modification strategy allow the control of platoons of vehicles affected by parameter mismatches and disturbances with bounded adaptive gains. However, the aforementioned methods do not ensure stability and performance against network imperfections (e.g. packet drop and/or communication delay) in wireless communication systems [13], [17]–[19]. Moreover, except for the method presented in [9], the aforementioned techniques do not consider *(ii)* vehicle uncertainties such as parametric uncertainty (i.e., vehicle mass, engine time constant etc. [20]), and *(iii)* external disturbances (e.g., lead vehicle's acceleration, wind gust or road slope [15], [20], [21] acting on the vehicles in a platoon). In the literature, researches have analysed the stability and performances for vehicle platoon systems considering packet drops [17], [22], communication delays [14], [23], [24], parametric uncertainties [20], [25] and external disturbances [15] either separately or by combining two or more factors [18], [21]. For example, effect of packet drops, and network access limitations have been analysed for homogeneous platoon by modeling vehicle platoon as discrete time switching system under packet drop rate in [17]. A decentralized model predictive controller (MPC) has been designed by considering a short-range wireless communication environment among platoon vehicles under low and high communication latency in [26]. Other approaches have used the concept of cooperative adaptive cruise control to analyse string stability and performances of a platoon under packet drops [17], [27] and communication delay [28], [29] for vehicles connected through wireless communication systems. The vehicle platoon control problem has been designed as a synchronisation problem of networked multi-agent systems with and without networked constraints (e.g. packet drop, communication delay etc.) in [14], [24], [30] and [9], [31], respectively, considering either algebraic graph theory and syncronisation of dynamical systems [9], [14] or both algebraic graph theory and concepts of networked control systems (NCS) [30] to maintain the cooperative platoon motion.

For the consensus problem of networked multi-agent systems, various controller design methodologies, e.g., MPC [16], [32], [33], state-feedback [34], [35], H_∞ controller [15], [18], [30] etc. have been investigated. For example, robust H_∞ controller has been designed for heterogeneous and autonomous multi-agent systems without network constraints and with time varying communication delay under undirected topology in [31] and [36], respectively. Event triggered

consensus has been investigated by designing the state-feedback controller for homogeneous multi-agent systems under undirected topology and packet drop modelled as Bernoulli distribution in [37]. State-feedback controller has been designed using LMI-based approach for the homogeneous multi-agent systems with undirected network topology under Bernoulii distributed packet drop in [34], [38], whereas LMI-based approach has been studied for average consensus problem of linear multi-agent system with undirected network topology under both time varying delays and random packet drop in [39]. Utilizing the concept of synchronisation problem of multi-agent systems, Tang *et al.* [22] have considered homogeneous platoons and have designed an LMI-based distributed state-feedback controller to achieve the coordinated vehicle motion under packet loss modelled as a Bernoulli distribution. The works presented in [22], [30], [34], [37]–[39] modelled random packet drops as a mean packet drop rate using Bernoulli probabilistic distribution and considered symmetric packet drop rate in the communication link for the synchronisation problem of multi agent system with undirected topology. In [14], a Lyapunov based design has been adopted to find out the maximum communication delay that preserves the consensus. For consensus control of heterogeneous platoon systems, a time-varying communication delay has been considered in [40] and both probabilistic packet drops and time-varying communication delays have been considered in [24]. However, amongst these controller design approaches, H_∞ controller has become popular due to its robustness and disturbance attenuation properties [15], [18], [30], [41]–[44] and references therein. For the homogeneous platoon control problem, stability and performance have been analysed by designing an LMI-based distributed H_∞ controller where packet drops were modelled by using both Bernoulli distributions and Markov chains [45]. A distributed H_∞ controller design has been proposed to ensure robustness and string stability for multi-vehicle systems with parametric uncertainty in [46]. By considering the external disturbances, an LMI-based distributed H_∞ controller has been designed for vehicle platoon systems in continuous-time domain with undirected topology in [15], where authors also provided an analytical derivation of a lower bound for the robustness measure γ-gain. Both the methods proposed in [15] and [46] do not analyse the stability and performances for vehicle platoon system under network imperfections such as packet drop and/or communication delays. However, the combination of all these issues (e.g., packet drop and/or communication delays, parametric uncertainty and/or external disturbances) is still a challenging research problem for the platoon control application [16], [19]. To best our knowledge, few researchers have proposed control strategies for vehicle platoon control with parametric uncertainty, external disturbances and packet drop and/or communication delay [18], [21], [29]. For example, an H_∞ controller has been designed for heterogeneous platoon systems under parametric uncertainty and uniform communication delays in [18]. An LMI-based distributed H_∞ controller has been designed for heterogeneous vehicle platoons under parametric uncertainties, external disturbances and bounded communication delays in [29] and for homogeneous platoons under external disturbances and stochastic communication delays in [47]. However, methods in [29], [47] only considered the PLF network topology for the communication among the platoon vehicles. Difference from [29], [47], this paper proposes a robust distributed H_∞ controller design methodology for homogeneous vehicle platoon systems for undirected network topologies which guarantees closed-loop stability and robustness to random single packet drop and external disturbances. In addition, this paper also provides an analytical understanding of the performance limitation of the vehicle platoon systems with undirected topology in terms of lower bound of the robustness measure (i.e., the γ-gain) under single packet drop which has not yet been investigated in the platoon literature. Hence, this work extends that presented in [15] where stability and robustness were analysed in terms of lower bounds for the γ-gain for homogeneous vehicle platoon systems without packet drops, i.e., only for perfect communication networks. Hence, the main contributions of this paper can be summarized as follow.

- An LMI-based distributed H_∞ controller ensuring mean square stability (MSS) is designed for homogenous vehicle platoons under random single packet drop modelled via Bernoulli probabilistic distributions. Similar to [15], [34], for undirected platoon topologies, a technique for reducing the LMI that guarantees the MSS stability of the entire platoon to an LMI condition on the dynamics of a single vehicle is found, thus reducing the computational complexity for the tuning of the distributed controller.
- For two undirected platoon topologies, namely BPF and BPLF, lower bounds for the robustness measure (i.e., the γ-gain) are derived from the perspective of energy amplification under external disturbances and random single packet drop in discrete time domain. Moreover, a lower bound of the γ-gain for undirected is analytically derived and related to the eigenvalues of the Laplacian and pinning matrices of the topology.
- An analytical and simulation study on the relation between the lower bounds on γ-gain and information exchanged between the platoon leader and platoon followers is also presented.

III. Vehicle Platoon Modeling and Control Objectives Under Random Packet Drop

This paper considers the vehicle platoon control problem as a synchronisation problem of networked dynamical systems with pinner node (i.e., the platoon leader) where a set of follower vehicles (i.e., nodes) interact through a communication network. These nodes are controlled in such a way that their dynamics converge towards those of the pinner node. The main components of a network of dynamical systems are *(i)* the individual node dynamics which describes the evaluation of each node when not coupled with the network; *(ii)* the network topology which describes the communication among nodes; and *(iii)* the control action to each node for steering the node dynamics to the pinner's trajectory. This section describes *(i)* the modeling of the platoon network topology and longitudinal vehicle dynamics which represent the node dynamics and *(ii)* the platoon control objectives.

In what follows, some mathematical notations used throughout the paper are introduced for the sake of completeness. $\mathbb{R}^n$ and $\mathbb{R}^{n\times n}$ are the n-dimensional real Euclidean space and the $n \times n$ real matrix space, respectively. $\boldsymbol{F}^T$ and $\boldsymbol{F}^{-1}$ denote the transpose and the inverse of a square matrix $\boldsymbol{F}$, respectively. $\boldsymbol{F} > \boldsymbol{0}$ ($\boldsymbol{F} < \boldsymbol{0}$) is a strictly positive (negative) definite matrix, whereas, $\boldsymbol{F} = \boldsymbol{F}^T \geq \boldsymbol{0}$ ($\boldsymbol{F} = \boldsymbol{F}^T \leq \boldsymbol{0}$) denotes a symmetric positive (negative) semi-definite matrix. $\lambda_i(\boldsymbol{F})$ is the i-th eigenvalue of a symmetric matrix $\boldsymbol{F}$ after they have been sorted in ascending order, and $\lambda_{\min}(\boldsymbol{F})$ denotes the minimum eigenvalue of $\boldsymbol{F}$. $\boldsymbol{I}_n$ is the unit matrix in the $n \times n$ real matrix space. For a matrix $\boldsymbol{\phi}$ with generic dimension, $\sigma_{\max}(\boldsymbol{\phi})$ is the maximum singular value of $\boldsymbol{\phi}$. The symbol $(*)$ represents the symmetric elements of a symmetric matrix. The symbol $(\otimes)$ represents the Kronecker product between two matrices. Given a random variable ξ, $\mathbb{E}(\xi)$ denotes its expected value (mean value).

A. Modeling of the Platoon Network Topology and Packet Drop

The communication topology of the N followers (nodes) can be represented by a graph $\mathcal{G}_N = (\mathcal{V}_N, \mathcal{E}_N)$, where $\mathcal{V}_N = \{1, 2, \ldots, N\}$ is the set of vertices or nodes and $\mathcal{E}_N \subseteq \mathcal{V}_N \times \mathcal{V}_N$ is the set of arcs or edges. The pair $(i, j) \in \mathcal{E}_N$ indicates that the i^{th} vehicle receives the information from the j^{th} vehicle. The adjacency matrix $\mathcal{A}_N = [a_{ij}] \in \mathbb{R}^{N\times N}$ is defined based on the edges $\mathcal{E}_N$. It is assumed that *(i)* $a_{ij} = 1$ when $(i, j) \in \mathcal{E}_N$ and $a_{ij} = 0$ otherwise, i.e., $a_{ij} = 1$ implies that the i^{th} vehicle receives information from the j^{th} vehicle, and *(ii)* $a_{ii} = 0$, thus there are no self-loop in the network. The degree matrix $\mathcal{D}_N$ is a diagonal matrix where the i^{th} entry on its diagonal represents the number of edges pointing to the i^{th} follower. The Laplacian matrix $\mathcal{L} = [l_{ij}] \in \mathbb{R}^{N\times N}$ is defined as $\mathcal{L} = \mathcal{D}_N - \mathcal{A}_N$, thus $l_{ii} = \sum_{j\neq i} a_{ij}$, and $l_{ij} = -a_{ij}$ $\forall$ $i \neq j$. $\mathbb{N}_i$ denotes the neighbour set of the node i, i.e., $\mathbb{N}_i = \{j \in \mathcal{V}_N \mid a_{ij} = 1\}$. The platoon follower vehicles may be connected to the leader and it is further assumed that all the followers may receive information from the leader. However, the followers will not send any information to the leader [6], [9], [15]. To systematically consider the leader (i.e., pinner of the network), the graph $\mathcal{G}_N$ is augmented with node 0 and the modified graph is denoted as $\mathcal{G}_{N+1} = (\mathcal{V}_{N+1}, \mathcal{E}_{N+1})$ where $\mathcal{V}_{N+1} = \{0, 1, \ldots, N\}$ and $\mathcal{E}_{N+1} \subseteq \mathcal{V}_{N+1} \times \mathcal{V}_{N+1}$, with the index 0 representing the leader node. The corresponding adjacency matrix is $\mathcal{A}_{N+1} = [a_{ij}] \in \mathbb{R}^{(N+1)\times(N+1)}$ with $a_{0j} = 0$, $j = 1, 2, \ldots, N$, indicates that the followers do not send information to the leader, $a_{i0} = 1$ indicates that the i^{th}-follower receives information from the leader otherwise $a_{i0} = 0$, $i = 1, 2, \ldots, N$. $\mathcal{P} = diag\{p_1, p_2, \ldots, p_N\}$ represents the pinning matrix which defines connection between each follower to the leader where $p_i = 1$ if node i is obtaining the information from the leader through wireless communications, i.e., node i is pinned to the leader, and $p_i = 0$, otherwise. The leader accessible set of node i is defined as:

$$\mathcal{P}_i = \begin{cases} \{0\} & \text{if } p_i = 1, \\ \emptyset & \text{if } p_i = 0. \end{cases} \tag{1}$$

This paper considers undirected topologies, i.e., $i \in \mathbb{N}_i \Leftrightarrow j \in \mathbb{N}_j$, $\forall i$, $j \in \mathcal{V}_N$. A spanning tree is a tree which connects all nodes of a graph [48] and for the rest of the paper the following assumption is supposed to hold.

Assumption 1 [15]: The leader is globally reachable to all the followers in the augmented graph $\mathcal{G}_{N+1}$, i.e., at least one spanning tree routing at the leader in the graph $\mathcal{G}_{N+1}$.

Assumption 1 guarantees that each follower receives information from the leader either directly or indirectly. This condition is required for ensuring the internal stability of a vehicle platoon and it is commonly assumed in the literature. Furthermore, as the undirected topologies are assumed, Assumption 1 also implies that the matrices $(\mathcal{L} + \mathcal{P})$ is positive definite as stated in the following Lemma.

Lemma 1 [49]: For any undirected topology $\lambda_{\min}(\mathcal{L}) = 0$ with the corresponding eigenvector $\mathbf{1}_N = [1, 1, \ldots, 1]^T \in \mathbb{R}^N$. Futhermore, as Assumption 1 holds, all the eigenvalues of $(\mathcal{L} + \mathcal{P})$ are greater than zero, i.e., $\lambda_i(\mathcal{L} + \mathcal{P}) > 0$, $i = 1, 2, \ldots, N$.

Lemma 1 is widely used in the synchronisation problem of multi-agent systems and vehicle platoon control solutions [4], [15], [34], [49] to analyse the closed-loop system under different network topologies [4], [8], [15].

For each pair of vehicles $(j, i) \in \mathcal{E}_N$, $\theta_{ij}(k) \in \{0, 1\}$ is a stochastic variable with a Bernoulli distribution which models the packet drop in the communication within the pair. When $\theta_{ji}(k) = 0$, the follower j receives the information (i.e., the packet) from the i^{th}-follower at the time instant k, while in the case $\theta_{ji}(k) = 1$ then the packet is lost. The following assumption is made:

$$Prob(\theta_{ji}(k) = 1) = \mathbb{E}(\theta_{ji}(k)) = r, \forall i \neq j, \tag{2a}$$

$$\mathbb{E}(1 - \theta_{ji}(k)) = 1 - r, \forall i \neq j, \tag{2b}$$

where, r is the mean packet drop rate of the communication network.

B. Modeling of the Longitudinal Vehicle Dynamics

For vehicle platooning applications, the longitudinal vehicle dynamics can be represented by a third order linear time invariant system which provides a satisfactory trade-off between accuracy and model complexity [4], [9], [15]. By defining the state of the i^{th}-vehicle as $\boldsymbol{x}_i^T(t) = [s_i, v_i, a_i]$, $i = 1, 2, \ldots, N$, where $\{s_i, v_i, a_i\}$ are its position, speed and acceleration, respectively, the longitudinal vehicle dynamics of the i^{th}-follower in a homogeneous platoon subjected to external disturbances are

$$\dot{\boldsymbol{x}}_i(t) = \boldsymbol{A}\boldsymbol{x}_i(t) + \boldsymbol{B}u_i(t) + \boldsymbol{B}w_i(t), \tag{3a}$$

$$y_i(t) = \boldsymbol{C}\boldsymbol{x}_i(t), \tag{3b}$$

where, $u_i(t) \in \mathbb{R}$, $w_i(t) \in \mathbb{R} \in L_2[0, \infty)$ and $y_i(t) \in \mathbb{R}$ are the system input, the exogenous disturbance, and output, respectively, while the system matrices are

$$\boldsymbol{A} = \begin{bmatrix} 0 & 1 & 0 \\ 0 & 0 & 1 \\ 0 & 0 & -\frac{1}{\tau} \end{bmatrix}, \quad \boldsymbol{B} = \begin{bmatrix} 0 \\ 0 \\ \frac{1}{\tau} \end{bmatrix}, \quad \boldsymbol{C} = \begin{bmatrix} 1 & 0 & 0 \end{bmatrix}, \tag{4}$$

with τ being the time lag of the powertrain.

The continuous time system (3) can be discretised by using the forward Euler discretisation method with sampling time T_s. Hence, the equivalent discrete time vehicle dynamics are

$$\boldsymbol{x}_i(k+1) = \boldsymbol{A}_d\boldsymbol{x}_i(k) + \boldsymbol{B}_d u_i(k) + \boldsymbol{B}_d w_i(k), \quad (5a)$$

$$y_i(k) = \boldsymbol{C}\boldsymbol{x}_i(k), \quad (5b)$$

where, $\boldsymbol{A}_d = \boldsymbol{I}_3 + \boldsymbol{A}T_s$ and $\boldsymbol{B}_d = \boldsymbol{B}T_s$ as reported in [50]–[52].

C. Platoon Control Objectives

The platoon control objective is twofold [9]: (*i*) to impose the leader's velocity to all followers and (*ii*) maintain a given inter-vehicular distance between consecutive platoon vehicles specified by a spacing policy [9], [15], [30]. If a constant spacing is adopted and $d_{i,i-1}$, $i = 1, 2, \ldots, N$ denotes the desired constant inter-vehicular distance between i^{th} vehicle and its predecessor, then the aim of the platoon control in deterministic scenarios (i.e., without random packet drops) is to find control law $u_i(k)$, $i = 1, 2, \ldots, N$ in (5) such that

$$\lim_{k\to\infty} \parallel v_i(k) - v_0(k) \parallel = 0, \quad (6a)$$

$$\lim_{k\to\infty} \parallel s_i(k) - s_{i-1}(k) - d_{i,i-1} \parallel = 0, \quad \forall i = 1, 2, \ldots, N, \quad (6b)$$

where, v_0 is the leader's velocity which can be assumed being a constant speed (i.e., $a_0(k) = 0$) [9], [15].

Notice that, by denoting $d_{i,0}$ the desired distance between the leader and the i^{th}-follower, i.e., $d_{i,0} = \sum_{m=1}^{i} d_{m,m-1}$, then the second objective (6b) can be re-written as $\lim_{k\to\infty} \parallel s_i(k) - s_0(k) - d_{i,0} \parallel = 0$ which together with the first objective (6a) represents a synchronisation problem where the leader acts as the pinner and provides the reference trajectory [9], [15]. Hence, by defining the tracking error for the follower i as $\hat{\boldsymbol{x}}_i(k) = [\hat{s}_i(k), \hat{v}_i(k), \hat{a}_i(k)]^T$, with $\hat{s}_i(k) = s_i(k) - s_0(k) - d_{i,0}$, $\hat{v}_i(k) = v_i(k) - v_0(k)$, $\hat{a}_i(k) = a_i(k) - a_0(k)$, conditions (6) becomes

$$\parallel \hat{\boldsymbol{x}}_i(k) \parallel \to 0 \quad \text{when} \quad k \to \infty, \quad \forall i = 1, 2, \ldots, N. \quad (7)$$

However, conditions (7) do not consider (*i*) the presence of the packet drops that might allow only the expected value of the tracking errors converge to zero as the time goes to infinite, and (*ii*) the effect of the external disturbances $w_i(t)$ on the dynamics of the output $y_i(t)$, $i = 1, 2, \ldots N$.

For these reasons, in this paper, the platoon control objectives under random packet drop scenarios and external disturbances are formulated in terms of MSS and bounded H_∞ norm for stochastic dynamical systems. By defining the state tracking error as $\boldsymbol{X}(k) = [\hat{\boldsymbol{x}}_1^T(k), \hat{\boldsymbol{x}}_2^T(k), \ldots, \hat{\boldsymbol{x}}_N^T(k)]^T$, and the output tracking error as $\boldsymbol{Y}(k) = [\hat{s}_1(k), \hat{s}_2(k), \ldots, \hat{s}_N(k)]^T = (\boldsymbol{I}_N \otimes \boldsymbol{C})\boldsymbol{X}(k)$, the platoon control objectives is to impose MSS and bounded H_∞ norm as defined below.

Definition 1 [34]: The tracking error $\boldsymbol{X}(k)$ is said to be MSS if $\lim_{k\to\infty} \mathbb{E}(\parallel \boldsymbol{X}(k) \parallel^2) = 0$ for any initial state $\boldsymbol{X}(0) \in \mathbb{R}^{3N}$.

Definition 2 [53]: The output error dynamics, $\boldsymbol{Y}(k)$, are said to have a bounded H_∞ norm $\gamma > 0$, when the closed-loop system is MSS and

$$\sum_{k=0}^{\infty} \mathbb{E}(\parallel \boldsymbol{Y}(k) \parallel^2) \leqslant \gamma^2 \sum_{k=0}^{\infty} \mathbb{E}(\parallel \boldsymbol{W}(k) \parallel^2), \quad (8)$$

for all $\boldsymbol{W}(k) \neq 0$ and $\boldsymbol{X}(0) = 0$ with $\boldsymbol{W}(k) = [w_1(k), w_2(k), \ldots, w_N(k)]^T$.

Remarks 1:

- Definition 1 requires that the expectation value of closed-loop state (tracking error) converges to zero to be MSS, i.e., $\lim_{k\to\infty} \mathbb{E}(\parallel \boldsymbol{X}(k) \parallel^2) = 0$, thus it is the counterpart of condition (7) in a stochastic framework.
- Definition 2 requires that the expectation value of disturbance input $\boldsymbol{W}(k)$ should be non-zero for the output $\boldsymbol{Y}(k)$ of a system to be bounded with an H_∞ norm $\gamma > 0$. Hence, Definition 2 provides a measure of robustness of the closed-loop system in terms of disturbance propagation in a stochastic framework [53].

IV. Platoon Controller Design Under Packet Drop

As in [30], [34], the control action in presence of random single packet drop is based on the following augmented states

$$\bar{\boldsymbol{x}}_j(k) = (1 - \theta_{ji}(k))\hat{\boldsymbol{x}}_j(k) + \theta_{ji}(k)\hat{\boldsymbol{x}}_j(k-1), \quad (9)$$

and

$$\bar{\boldsymbol{x}}_i(k) = (1 - \theta_{ij}(k))\hat{\boldsymbol{x}}_i(k) + \theta_{ij}(k)\hat{\boldsymbol{x}}_i(k-1), \quad (10)$$

where, $\bar{\boldsymbol{x}}_j(k)$ represents tracking error for the j^{th} vehicle that the i^{th} vehicle can use at time instant kT_s as the i^{th}-vehicle knows whether the information packet from j^{th}-vehicle has been received or not. It is noted that r is the mean packet drop rate in the communication network as detailed in Section. III. As in [22], [30], [34], [37]–[39], it is assumed that $\theta_{ji}(k) = \theta_{ij}(k)$, thus a link failure affects the packet drop in both directions.

The distributed control action for each follower is a static full state-feedback action based on the augmented states (9)-(10) as that presented in [30], [34], i.e.,

$$u_i(k) = \boldsymbol{K} \sum_{j\in\mathbb{Q}_i} (\bar{\boldsymbol{x}}_i(k) - \bar{\boldsymbol{x}}_j(k)), \forall i = 1, 2, \ldots, N, \quad (11)$$

where, $\mathbb{Q}_i = \mathbb{N}_i \cup \mathcal{P}_i$ is the neighbour set of the i^{th}-follower in the $\mathcal{G}_{N+1}$ graph and $\boldsymbol{K} = [-K_s, -K_v, -K_a]$ is the control gain assumed to be identical for each follower as the platoon is homogeneous [15], [30].

Now, defining the augmented states $\boldsymbol{U}(k) = [u_1(k), u_2(k), \ldots, u_N(k)]^T$, the stack of control actions, the assumption of undirected network topology implies,

$$\boldsymbol{U}(k) = (\mathcal{L} + \mathcal{P}) \otimes \boldsymbol{K}[(1 - \theta_{ij}(k))\boldsymbol{X}(k) - (\theta_{ij}(k))\boldsymbol{X}(k-1)]. \quad (12)$$

Furthermore, when the control law (12) is applied to a homogeneous platoon with vehicle dynamics (5) under packet

drop scenarios, the closed-loop dynamics of the state tracking error are

$$\begin{aligned} \boldsymbol{X}(k+1) &= (\boldsymbol{I}_N \otimes \boldsymbol{A}_d)\boldsymbol{X}(k) + ((\mathcal{L}+\mathcal{P})(1-\theta_{ij}(k)) \\ &\quad \otimes \boldsymbol{B}_d\boldsymbol{K})\boldsymbol{X}(k) + ((\mathcal{L}+\mathcal{P})\theta_{ij}(k) \otimes \boldsymbol{B}_d\boldsymbol{K}) \\ &\quad \times \boldsymbol{X}(k-1) + (\boldsymbol{I}_N \otimes \boldsymbol{B}_d)\boldsymbol{W}(k), \\ \boldsymbol{Y}(k) &= (\boldsymbol{I}_N \otimes \boldsymbol{C})\boldsymbol{X}(k). \end{aligned} \tag{13}$$

The only control parameter in (12) that has to be tuned to imposed the required control objectives to system (13) is the control gain $\boldsymbol{K}$. In this paper, an LMI-based approach is used to provide sufficient conditions for the design of the control gain $\boldsymbol{K}$ such that system (13) is MSS and has a bounded H_∞ norm (see also Definition 1 and 2).

Theorem 1: The closed-loop system (13) with packet drop modelled as in (2) with mean packet drop rate r is MSS with a bounded H_∞ norm γ if there exist $\boldsymbol{P} = \boldsymbol{P}^T = \boldsymbol{I}_N \otimes \boldsymbol{P}_0 > \boldsymbol{0} \in \mathbb{R}^{3N\times 3N}$, $\boldsymbol{Q} = \boldsymbol{Q}^T = \boldsymbol{I}_N \otimes \boldsymbol{Q}_0 > \boldsymbol{0} \in \mathbb{R}^{3N\times 3N}$ and $\boldsymbol{Z} \in \mathbb{R}^{1\times 3}$ such that $\boldsymbol{\Xi}_1 < \boldsymbol{0}$ (in (14), shown at the bottom of the page), and

$$\boldsymbol{\Xi}_2 = \begin{bmatrix} -\boldsymbol{M} & \bar{\boldsymbol{P}} \\ * & -\bar{\boldsymbol{Q}} \end{bmatrix} \leq \boldsymbol{0}. \tag{15}$$

where, $\boldsymbol{P}^{-1} = \bar{\boldsymbol{P}}$, $\boldsymbol{Q}^{-1} = \bar{\boldsymbol{Q}}$, $\boldsymbol{P}^{-1}\boldsymbol{Q}\boldsymbol{P}^{-1} = \boldsymbol{M} = \boldsymbol{I}_N \otimes \boldsymbol{M}_0$, $\tilde{\boldsymbol{L}} = (\mathcal{L}+\mathcal{P})$ and the controller gain (12) is selected as $\boldsymbol{K} = \boldsymbol{Z}\bar{\boldsymbol{P}}_0{}^{-1} = \boldsymbol{Z}\boldsymbol{P}_0 \in \mathbb{R}^{1\times 3}$.

The LMI in Theorem 1 has a high dimension for a large number of platoon followers (e.g., $\boldsymbol{\Xi}_1 \in \mathbb{R}^{15N\times 15N}$ and $\boldsymbol{\Xi}_2 \in \mathbb{R}^{6N\times 6N}$) which may require high computation effort and can result in an intractable and/or unfeasible problem. To improve the efficiency of the computation, the concept of orthogonally as that presented in [34] can be used for decomposing inequality (14) as stated in the following Theorem which provides an alternative approach for computing the control gain.

Theorem 2: The closed-loop system (13) with packet drop modelled as in (2) with mean packet drop rate r is MSS with a bounded H_∞ norm γ if there exist $\boldsymbol{P}_0 = \boldsymbol{P}_0{}^T > \boldsymbol{0} \in \mathbb{R}^{3\times 3}$, $\boldsymbol{Q}_0 = \boldsymbol{Q}_0{}^T > \boldsymbol{0} \in \mathbb{R}^{3\times 3}$ and $\boldsymbol{Z} \in \mathbb{R}^{1\times 3}$ for which the following matrix inequalities hold $\forall\ \lambda_i \triangleq \lambda_i(\mathcal{L}+\mathcal{P})$, $i = 1, 2, \ldots, N$:

$$\tilde{\boldsymbol{\Xi}}_1^i = \begin{bmatrix} \boldsymbol{M}_0 - \bar{\boldsymbol{P}}_0 & * & * & * & * \\ \boldsymbol{0} & -\boldsymbol{M}_0 & * & * & * \\ \boldsymbol{0} & \boldsymbol{0} & -\gamma^2\boldsymbol{I}_1 & * & * \\ (\boldsymbol{A}_d\bar{\boldsymbol{P}}_0 + \lambda_i(1-r)\boldsymbol{B}_d\boldsymbol{Z}) & \lambda_i r\boldsymbol{B}_d\boldsymbol{Z} & \boldsymbol{B}_d & -\bar{\boldsymbol{P}}_0 & * \\ \boldsymbol{C}\bar{\boldsymbol{P}}_0 & \boldsymbol{0} & \boldsymbol{0} & \boldsymbol{0} & -\boldsymbol{I}_1 \end{bmatrix} < \boldsymbol{0}, \tag{16}$$

$$\tilde{\boldsymbol{\Xi}}_2 = \begin{bmatrix} -\boldsymbol{M}_0 & \bar{\boldsymbol{P}}_0 \\ * & -\bar{\boldsymbol{Q}}_0 \end{bmatrix} \leq \boldsymbol{0}, \tag{17}$$

where, $\boldsymbol{P}_0{}^{-1} = \bar{\boldsymbol{P}}_0$, $\boldsymbol{Q}_0{}^{-1} = \bar{\boldsymbol{Q}}_0$, $\boldsymbol{P}_0{}^{-1}\boldsymbol{Q}_0\boldsymbol{P}_0{}^{-1} = \boldsymbol{M}_0$, and the controller gain (12) is selected as $\boldsymbol{K} = \boldsymbol{Z}\bar{\boldsymbol{P}}_0{}^{-1} = \boldsymbol{Z}\boldsymbol{P}_0 \in \mathbb{R}^{1\times 3}$.

Remarks 2:

- The dimension of the set of LMIs (14)-(15) scales with the number of platoon followers. Hence, for platoon systems with large number of follower vehicles, the solution of such LMIs can become computationally intractable. Consequently, the LMIs in (14)-(15) are decomposed for individual vehicles to obtain the LMIs in (16)-(17).
- As $\{\tilde{\boldsymbol{\Xi}}_1^i,\ \tilde{\boldsymbol{\Xi}}_2\}$, $i = 1, 2, \ldots, N$, are affine in λ_i, the set of LMIs (16)-(17) holds if and only if it holds for the maximum and minimum eigenvalues of $(\mathcal{L}+\mathcal{P})$ [34]. Hence, the set of LMIs (16)-(17) does not depend on the number of platoon followers.
- Inequalities (14) and (15) can be relaxed as presented in [30], to facilitate their solutions.

The analytical proofs of Theorem 1 and Theorem 2 are reported in Appendix B and C, respectively.

V. Robustness Analysis for Vehicle Platoon Under Packet Drop

This section describes robustness analysis of a vehicle platoon system with an undirected network topology under random packet drops. The lower bound for generic undirected topologies is then tailored for two topologies, i.e., BPF and BPLF topologies (see also shown Fig. 1 for a schematic representation of such topologies), which are common undirected topologies [15]. For both BPF and BPLF topologies, the adjacency matrix $\mathcal{A}_N = [a_{ij}] \in \mathbb{R}^{N\times N}$ has entries $a_{ij} = 1$, $a_{N,N-1} = 1$, $a_{i,i-1} = 1$, $a_{1,i+1} = 1$, $i = 2, \ldots, N-1$ and 0 elsewhere. The pinning matrix $\mathcal{P}$ has entries $p_1 = 1$, $p_i = 0$, $i = 2, \ldots, N$ in the case of the BPF, and $p_i = 1, i = 1, \ldots, N$ for the BPLF.

A. Robust Performance Measures γ Gain

The robustness measure γ-gain is derived from the perspective of energy amplification under external disturbances and random packet drops. We consider bounded external disturbances $\boldsymbol{W}(k) \in \mathbb{R}^N$ which act on the acceleration of each vehicle and have a finite energy, thus $\boldsymbol{W} \in L_2 \in [0, \infty)$, i.e., $\mathbb{E}\{\|\ \boldsymbol{W}\ \|_{L_2}\} = \sum_{k=0}^{\infty}\mathbb{E}\{\boldsymbol{W}^T(k)\boldsymbol{W}(k)\} < +\infty$ [53]. This disturbances effect the inter-vehicular spacing error of the platoon follower $\boldsymbol{Y}(k) \in \mathbb{R}^N$ in the form of energy amplification [15], [53]. In this framework, the γ-gain is used to quantify how the distrubance propagates through the system output, and thus it provides a measurement of the robustness of platoon as to external disturbances and it is defined as follows.

Definition 3 [15], [41], [53]–[55]: For the homogeneous platoon (13) the γ-gain representing amplification factor is

$$\boldsymbol{\Xi}_1 = \begin{bmatrix} \boldsymbol{M} - \bar{\boldsymbol{P}} & * & * & * & * \\ \boldsymbol{0} & -\boldsymbol{M} & * & * & * \\ \boldsymbol{0} & \boldsymbol{0} & -\gamma^2\boldsymbol{I}_N & * & * \\ ((\boldsymbol{I}_N \otimes \boldsymbol{A}_d)\bar{\boldsymbol{P}} + \tilde{\boldsymbol{L}}(1-r) \otimes \boldsymbol{B}_d\boldsymbol{Z}) & \tilde{\boldsymbol{L}}r \otimes \boldsymbol{B}_d\boldsymbol{Z} & \boldsymbol{I}_N \otimes \boldsymbol{B}_d & -\bar{\boldsymbol{P}} & * \\ (\boldsymbol{I}_N \otimes \boldsymbol{C})\bar{\boldsymbol{P}} & \boldsymbol{0} & \boldsymbol{0} & \boldsymbol{0} & -\boldsymbol{I}_N \end{bmatrix} < \boldsymbol{0}. \tag{14}$$

defined as:

$$\gamma = \sup_{\|\boldsymbol{W}\|_{L_2}\neq 0} \frac{\mathbb{E}\{\| \boldsymbol{Y} \|_{L_2}\}}{\mathbb{E}\{\| \boldsymbol{W} \|_{L_2}\}}. \tag{18}$$

The sensitivity of the platoon control system to external disturbances with finite energy is analysed through (18). It is possible to prove that the γ - gain is equal to H_∞ norm of the transfer function $G(z)$ of closed-loop system (13) [41], thus

$$\gamma = \| G(z) \|_{H_\infty} = \sup_{\omega}[\sigma_{max}(G(e^{j\omega T_s}))]. \tag{19}$$

Identity (19) and the possibility of diagonalising the matrix $(\mathcal{L}+\mathcal{P})$ for undirected topologies are used in Appendix D and E to prove the results on the γ -gain presented in the next subsection.

B. Scaling Trend of the γ -Gain for Vehicle Platooning With Undirected Topologies and Under Packet Drop

For generic undirected topologies, a lower bound of the γ -gain under random packet drops is given by the following Theorem.

Theorem 3: Given the homogeneous closed-loop platoon system (13) with an undirected topology under random single packet drop, the γ -gain in (18) satisfies

$$\gamma \geq \frac{1}{\lambda_{min}(\mathcal{L}+\mathcal{P})K_s}, \tag{20}$$

where, K_s is the first entry of the control gain $\boldsymbol{K}$ in (12).

The lower bound in (20) can be tailored by upper bounding $\lambda_{min}(\mathcal{L}+\mathcal{P})$ as shown in Appendix E to prove the following corollaries. These Corollaries can be used to study the effect of the number of homogeneous follower vehicles and the connectivity to the platoon leader on the γ -gain.

Corollary 1: Given the homogeneous closed-loop platoon system (13) with an undirected topology under random single packet drop, the γ -gain satisfies

$$\gamma \geq \gamma^{\dagger} = \frac{N}{\Omega(N)K_s}, \tag{21}$$

where, $\Omega(N)$ represents the number of followers that are pinned to the leader and N is the number of followers in the platoon.

Next, Theorem 3 can be used to further tailor a lower bound of the γ -gain of a homogeneous platoon for the BPF and BPLF topologies under random packet drops as detailed in Corollaries 2 and 3, respectively.

Corollary 2: Given the homogeneous closed-loop platoon system (13) with a BPF topology under random single packet drop, the γ -gain satisfies

$$\gamma \geq \gamma^{\star}_{BPF} = \frac{N^2}{\pi^2 K_s}, \tag{22}$$

Corollary 3: Given the homogeneous closed-loop platoon system (13) with a BPLF topology under random single packet drop, the γ -gain satisfies

$$\gamma \geq \gamma^{\star}_{BPLF} = \frac{N^2}{(N^2+\pi^2)K_s}. \tag{23}$$

The proof of Theorem 3 and Corollaries 1, 2 and 3 are presented in Appendix D and E, respectively. It is interesting to point out that the lower bounds provided by Theorem 3 and Corollaries 1, 2 and 3 are those found in [15] for homogeneous vehicle platoons with an undirected topology in the continuous-time case but with a perfect communication network. However, as this work considers platoons in the discrete-time domain and under random packet drops, the transfer function (19) is different from that in [15], thus the lower bounds need to be computed in this case. From the above corollaries the following remarks can be derived which are similar to those in [15].

Remark 3: From Corollary 1, it can be observed that when more followers are connected to leader (i.e., a larger $\Omega(N)$ value), the lower bound reduces. Furthmore, the lower bound of the robustness measure for the BPLF topology is smaller than that for the BPF topology. This supports the intuitive rationale presented in [15] which stated that sharing of leader's trajectory information with a large number of platoon followers help in improving the local follower's behaviour in tracking the leader's trajectory also in presence of network imperfections (such as packet drop). It can be also observed from the Corollary 1 that the rate of growth of γ denoted as $\Theta(N)$ increases at least as $\mathcal{O}(N)$ for the BPF topology (with $\Omega(N)=1$) while this rate is an $\mathcal{O}(1)$, i.e., $\Theta(N)\in\mathcal{O}(1)$, for the BPLF topology ($\Omega(N)=N$). Moreover, the lower bound computed with Corollary 3 converges to that computed through Corollary 1 for the BPLF topology when N increases. Furthermore, Corollary 2 improves that scaling factor for the γ -gain when the BPF topology is used, as it shows that the γ -gain will increase as $\mathcal{O}(N^2)$.

Remark 4: In the case of the BPF topology, Corollary 1 provides a smaller lower bound of robustness measure γ -gain compared to Corollary 1 for any given controller gain (K_s) and number of followers in the platoon, especially, for large number of N. In the case of the BPLF, Corollary 3 always provides tighter lower bound of robustness measure γ -gain as compared to Corollary 1 and Corollary 2. Finally, the lower bound for the γ -gain provided by the BPF is always larger than that provided by the BPLF.

VI. Numerical Analysis and Simulation and Results

This section shows the effectiveness of the methodology for achieving the cooperative platoon when BPF and BPLF topology are used under random packet drops. The vehicle dynamics of the followers are assumed to be homogeneous [15] with a time-lag $\tau = 0.4$ s [8], [9], [30]. Furthermore, the continuous time system (3) is discretized as (5) with a sampling time $T_s = 0.1$ s [16], [55]. In Section. VI-A, the effect of the number of followers N and the mean packet drop rate r on the γ -gain is analysed, while in Section. VI-B simulation results in time domain are shown to confirm the ability of platoon controller to steer the dynamics of the followers toward those of the platoon leader.

A. Analysis of the γ Gain

The γ -gain measuring the closed-loop robustness in agreement with (19) has been computed by using inequalities

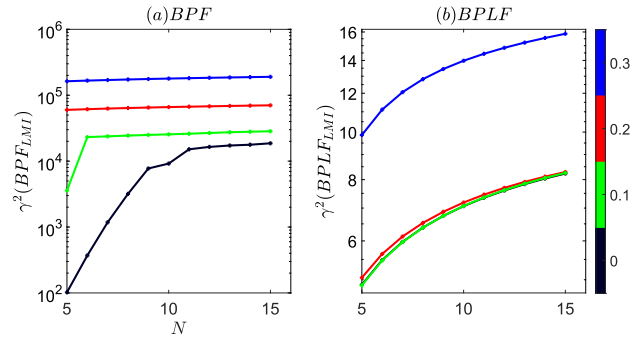

Fig. 2. Trend of the γ^2 with different number of follower vehicles and under varying packet drop rate (from 0% to 30%) for (a) the BPF topology and (b) the BPLF topology.

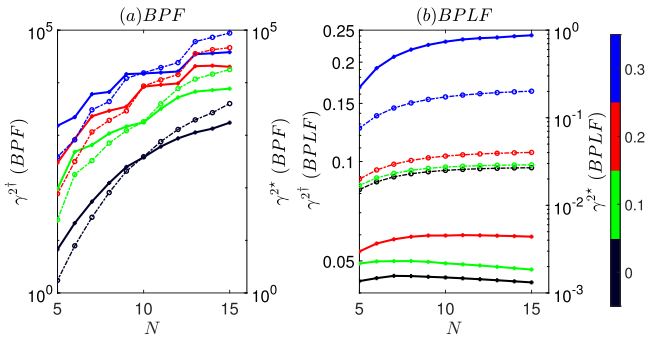

Fig. 3. Analytical lower bounds of the γ^2-gain with different number of follower vehicles under varying packet drop rate (from 0% to 30%) for (a) the BPF topology by using $\gamma^{\dagger 2}$ (solid line) in (21) and $\gamma^{\star 2}_{BPF}$ (dotted line) in (22); and (b) the BPLF topology by using $\gamma^{\dagger 2}$ (solid line) in (21) and $\gamma^{\star 2}_{BPLF}$ (dotted line) in (23).

(16)-(17), in the following optimisation problem

$$\begin{aligned} &\min \gamma \quad , \\ &\bar{\boldsymbol{P}}_0, \bar{\boldsymbol{Q}}_0, \boldsymbol{M}_0, \boldsymbol{Z}, \gamma \\ &s.t.\ (16) \text{ and } (17). \end{aligned}$$

This optimisation problem can be solved using available toolboxes in the MATLAB environment. The YALMIP toolbox [56], [57] has been used in this work as it provides a proven and general framework for solving large scale optimisation problems and can be combined with the SeDuMi solver [58] for its performance and ability to solve complex optimisation problems efficiently (e.g., the computation of the control gains for large vehicle platoon systems). The effect of the topology (BPF and BPLF), number platoon followers ($N = 5, \ldots, 15$) and packet drop rate ($r = 0, 0.1, 0.2, 0.3$, i.e., from no drop to 30% packet drop) on the trend of squared value of γ is shown in Fig. 2. From Fig. 2 emerges for any N-value, when packet drop rate increases, then the γ^2-gain obtained from LMIs (16) and (17) increases for both the BPF Fig. 2 (left panel) and BPLF topologies Fig. 2 (right panel). Similarly, for any value of the packet drop rate, the γ^2-gain increases when the number of platoon followers (N) increases. The higher γ^2-gain implies a decrease in robustness. Furthermore, Fig. 2 shows that the gain γ^2 is always higher for BPF topology when compared to the gain for the BPLF topology under identical network constraints (i.e., packet drop rate) and number of followers in the platoon, thus confirming the importance of the leader information to improve closed-loop robustness. Fig. 2 also provides a visual representation of the Remark 3 for both the BPF and BPLF topologies.

To demonstrate the tighter lower bound provided by (22) and (23) with respect to (21) and show the effect of leader information to the followers on the closed-loop robustness under varying packet drop rates and number of follower vehicles, the scaling trend of lower bounds for the γ^2-gain analytically computed through (21), (22) and (21), (23) for the BPF and BPLF topologies are shown in Fig. 3a and Fig. 3b, respectively. Notice that, for the BPF, the value of $\Omega(N) = 1$ and for the BPLF $\Omega(N) = N$. Similar to the results presented in Fig. 2, Fig. 3 shows an increasing trend of γ^2 when either the number of followers or the rate rate of packet drops increase. Furthermore, for the BPF topology, Fig. 3a confirms that the trend of γ^2 obtained from (22) is higher than the analytical expressions provided by (21), thus expression (22) gives a better prediction of a lower bound of bound of γ^2-gain. Fig. 3b shows that the analytical expressions (21) and (23) for the BPLF topology provide smaller lower bounds of γ^2-gain as compared to the analytical expressions (21) and (22) for packet drop rate as discussed in Remark 4. Moreover, the comparison of the trend of γ^2-gains in trend of γ^2-gains in Fig. 3a and Fig. 3b further confirms that BPLF topology is more robust as it always provides smaller γ^2-gains. This was expected as the leader information is sent to all the followers in the case of the BPLF topology but Fig. 3 provides a quantitative analysis of this feature.

B. Time-Based Simulation Analysis

For the time based simulations, the desired spacing is set to $d_{i,i-1} = 25\,\text{m}$ and 10 followers are considered. The initial vehicle states are chosen randomly. However, the maximum initial position mismatch among consecutive follower, i.e., $(e_{i,i-1}(k) = s_i(k) - s_{i-1}(k) - d_{i,i-1})$, is limited to 3 m, thus guaranteeing no vehicle collisions at the initial time $t = 0\,\text{s}$. Furthermore, the same initial states are used for the BPF and BPLF topologies. The leader's speed is constant at 72km h^{-1} [4], [9], [29]. The external disturbance input to the acceleration of all the followers is a single square wave (i.e., Heaviside function) with amplitude one, starting at $t = 500\,\text{s}$ and with duration 5 s, thus ensuring a limited energy, i.e., a bounded L_2 norm $\| w_i(k) \|_{L_2}$.

For both topologies, a 30% of random packet drop is considered. By solving the LMIs (16)-(17), the controller gains $\boldsymbol{K} = -[0.0817, 0.6793, 0.2587]$ and $\boldsymbol{K} = -[2.0820, 3.7923, 1.2232]$ are obtained for the BPF and the BPLF topology, respectively. The corresponding value of γ-gains obtained with LMIs (16)-(17) are $\gamma_{BPF} = 423.1194$ and $\gamma_{BPLF} = 3.7388$ for the BPF and BPLF topology, respectively. As expected these values are larger than the lower bounds provided by Corollary 2 and Corollary 3 which provide $\gamma^{\star}_{BPF} = 124.0484$ as lower bound for the BPF topology, and a lower bound of $\gamma^{\star}_{BPLF} = 0.4158$ for the BPLF topology, respectively.

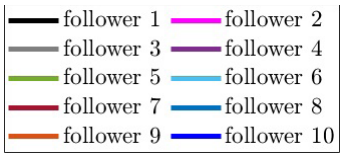

Fig. 4. Legend for Figs. 5, 6 and 7.

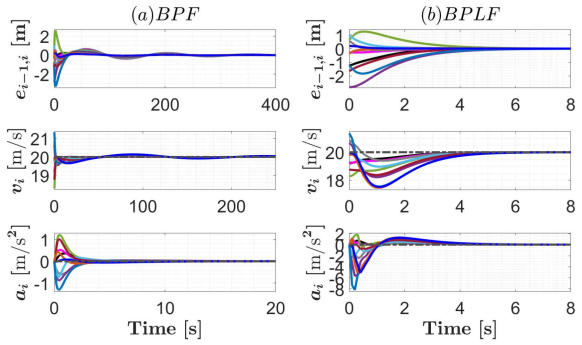

Fig. 5. Initial transient response for 10 follower vehicles (see colour legend in Fig. 4) under 30% packet drop rate when the topology is (a) the BPF (left panel) and (b) BPLF (right panel). The grey dotted line is the leader's velocity/acceleration.

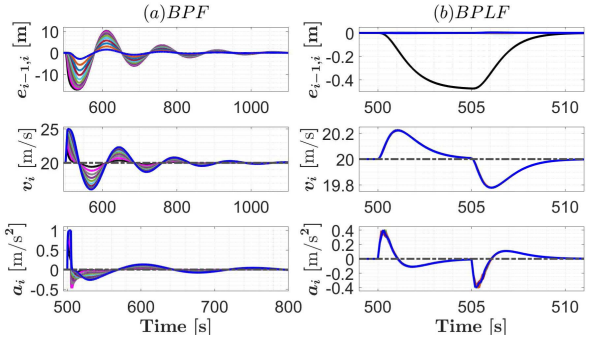

Fig. 6. Closed-loop response to transient disturbance for 10 follower vehicles (see colour legend in Fig. 4) under 30% packet drop rate when the topology is (a) the BPF (left panel) and (b) BPLF (right panel). The grey dotted line is the leader's velocity/acceleration.

The color legend for the following analysis in the time domain is shown in Fig. 4. Fig. 5 shows that when the control system is activated the vehicle dynamics of the followers converge to the cooperative platoon motion, i.e., zero inter-vehicular distance error, matching to leader's velocity, and zero accelerations. Furthermore, the converging time to the cooperative motion reduces when the BPLF topology is used instead of the BPF topology as the leader reference is sent to all the followers. followers. Fig. 6 shows the behaviour of follower's states when the external disturbances is follower. The resulting inter-vehicular distance error and the time for recovering the platoon motion are larger when the BPF topology is used (e.g., the maximumin inter-vehicular distance error is of 17 m in the case of the BPF topology). A better closed-loop rejection of disturbance is obtained when BPLF topology is used, as it provides a maximum inter-vehicular distance error of about 0.5 m and a time for re-establishing vehicle platooning of about 4 s. Furthermore, for BPLF topology the

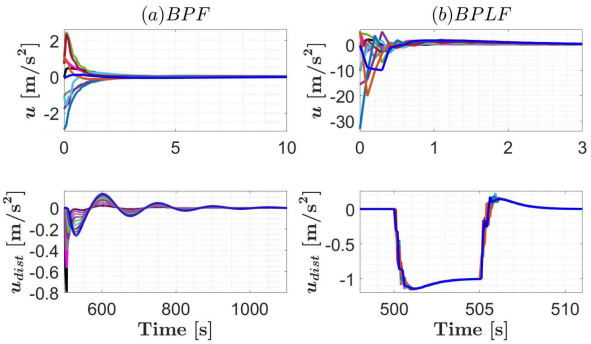

Fig. 7. Control inputs for 10 follower vehicles (see colour legend in Fig. 4) under 30% packet drop rate during the initial transient (upper panel) and when the external disturbance is applied (lower panel) in the case of (a) the BPF topology (left panel) and (b) the BPLF topology (right panel).

largest inter-vehicular distance error is always between the leader and the first follower, while for the other followers the position errors are negligible since all the followers have zero initial error (at steady state) before applying the disturbance and they are also pinned to the leader, thereby maintaining same dynamic evolution [4]. It is noted that the amplification of velocity errors is higher for BPF topology when compared to BPLF topology. Moreover, all the followers almost maintain the same velocity and acceleration when BPLF topology is used.

Finally, Fig. 7 depicts the control actions of on-board controllers and confirms that all the control inputs converges to zero for both topologies before the disturbance is applied and after it is rejected. Fig. 7 also shows that the control inputs have larger oscillations for the platoon system with the BPF topology when compared to those provided by the BPLF topology, especially during the application of the external disturbance. Hence, higher control efforts are required when the BPF topology is selected instead of the BPLF topology.

VII. Conclusion

In this paper, an LMI-based distributed state-feedback controller satisfying bounded H_∞ norm has been designed for homogeneous vehicle platoons under random single packet drop. The proposed design can consider different undirected network topologies, leader-to-follower connection strategies, and network imperfections. Lower bounds of the γ-gain, which provides a robustness measure of the closed-loop system to L_2 norm bounded disturbances, were analytically derived for the platoon system with undirected topology under random packet drops. The scaling trend of the bounded H_∞ norm γ for two platoon network topologies, i.e., the BPF and BPLF, as a function of the number of platoon followers under varying random packet drop has been also analytically investigated. The proposed controller was numerically validated in a simulation environment when the platoon followers are operated with BPF/BPLF network topologies and under random single packet drop. Simulation results demonstrated the effectiveness of the proposed controller to maintain the required platoon motion. Furthermore, the simulation analysis shown that better performance can be achieved when leader is connected to

all the followers (i.e., when BPLF topology is used instead of the BPF topology) in terms of maximum inter-vehicular error and rejection time of L_2-norm bounded disturbances. As part of future research, the robustness measures γ-gain will be investigated for vehicle platoons under undirected topologies to obtain a general-purpose H_∞ platoon control solution. Moreover, the LMI design to analyse stability and robustness measures γ-gain for the platoon systems under both undirected and directed topologies will be extended to accommodate multiple packet drop, variable time delays and asymmetric packet drop rate.

APPENDIX

Before presenting the proof of the main Theorems and Corollaries, the closed-loop dynamics (13) is converted into expected value dynamics due to presence of probabilistic random packet drop and the related transfer function is presented and used in the proof of Theorem 3.

A. Closed-Loop Expected Value Dynamics and Its Transfer Function

By using (2) and applying the expectation value to the closed-loop system (13), the expected value of the closed-loop dynamics is

$$\begin{aligned}\mathbb{E}(\boldsymbol{X}(k+1)) &= ((\boldsymbol{I}_N \otimes \boldsymbol{A}_d) + ((\mathcal{L}+\mathcal{P})(1-r) \otimes \boldsymbol{B}_d\boldsymbol{K})) \\ &\quad \times \mathbb{E}(\boldsymbol{X}(k)) + ((\mathcal{L}+\mathcal{P})r \otimes \boldsymbol{B}_d\boldsymbol{K})\mathbb{E}(\boldsymbol{X}(k-1)) \\ &\quad + (\boldsymbol{I}_N \otimes \boldsymbol{B}_d)\mathbb{E}(\boldsymbol{W}(k)), \\ \boldsymbol{Y}(k) &= (\boldsymbol{I}_N \otimes \boldsymbol{C})\mathbb{E}(\boldsymbol{X}(k)). \end{aligned} \tag{24}$$

Now, let $\boldsymbol{\eta}(k) = \boldsymbol{X}(k-1)$ be the state for the unit delay, the augmented closed-loop state is $\tilde{\boldsymbol{X}}(k) = [\boldsymbol{X}^T(k), \boldsymbol{\eta}^T(k)]^T$, whose the mean value dynamics obtained from (24) are

$$\begin{aligned}&\mathbb{E}(\tilde{\boldsymbol{X}}(k+1)) \\ &= \begin{bmatrix} (\boldsymbol{I}_N \otimes \boldsymbol{A}_d) + (\mathcal{L}+\mathcal{P})(1-r) \otimes \boldsymbol{B}_d\boldsymbol{K} & (\mathcal{L}+\mathcal{P})r \otimes \boldsymbol{B}_d\boldsymbol{K} \\ \boldsymbol{I}_{3N\times 3N} & \boldsymbol{0}_{3N\times 3N} \end{bmatrix} \\ &\quad \times \mathbb{E}(\tilde{\boldsymbol{X}}(k)) + \begin{bmatrix} \boldsymbol{I}_N \otimes \boldsymbol{B}_d \\ \boldsymbol{0}_{3N\times N} \end{bmatrix} \mathbb{E}(\boldsymbol{W}(k)). \end{aligned} \tag{25}$$

Now, with the assumption of zero initial tracking error, the transfer function from $\mathbb{E}(\boldsymbol{W}(k))$ to $\mathbb{E}(\boldsymbol{Y}(k))$ is (26) which is shown on the bottom of the page.

B. Proof of Theorem 1

By defining the Lyapunov function candidate as:

$$V(k) = \boldsymbol{X}^T(k)\boldsymbol{P}\boldsymbol{X}(k) + \boldsymbol{X}^T(k-1)\boldsymbol{Q}\boldsymbol{X}(k-1), \tag{27}$$

where, $\boldsymbol{P} = \boldsymbol{P}^T > \boldsymbol{0}$ and $\boldsymbol{Q} = \boldsymbol{Q}^T > \boldsymbol{0}$, the aim is to show that the LMIs in (14)-(15) are sufficient conditions for imposing

$$V(k+1) - V(k) + \boldsymbol{Y}^T(k)\boldsymbol{Y}(k) - \gamma^2\boldsymbol{W}^T(k)\boldsymbol{W}(k) < \boldsymbol{0}, \tag{28}$$

which is the condition required for having a bounded H_∞ norm γ in accordance with bounded real lemma (BRL) [53]–[55]. Now, by taking expectation value of (28), the following holds [53]:

$$\mathbb{E}\{\Delta V(k)\} + \mathbb{E}\{\boldsymbol{Y}^T(k)\boldsymbol{Y}(k) - \gamma^2\boldsymbol{W}^T(k)\boldsymbol{W}(k)\} < \boldsymbol{0}, \tag{29}$$

where, $\Delta V(k) = V(k+1) - V(k)$.

By replacing (25) in (29) and recalling from (2) that $\mathbb{E}(\theta_{ij}(k)) = r$ and $\mathbb{E}(1-\theta_{ij}(k)) = 1-r$, the expected value of the variation of the Lyapunov function in (29) can be written as in (30) which is shown on the bottom of the page, with $\bar{\boldsymbol{A}}_d = \boldsymbol{I}_N \otimes \boldsymbol{A}_d + (\mathcal{L}+\mathcal{P})(1-r) \otimes \boldsymbol{B}_d\boldsymbol{K}$, and $\tilde{\boldsymbol{L}} = (\mathcal{L}+\mathcal{P})$.

As in [53],

$$\begin{aligned}&\mathbb{E}\{(\boldsymbol{Y}^T(k)\boldsymbol{Y}(k) - \gamma^2(\boldsymbol{W}^T(k)\boldsymbol{W}(k))\} \\ &= \mathbb{E}\begin{bmatrix}\boldsymbol{X}^T(k) & \boldsymbol{X}^T(k-1) & \boldsymbol{W}^T(k)\end{bmatrix} \\ &\quad \times \begin{bmatrix} (\boldsymbol{I}_N \otimes \boldsymbol{C})^T(\boldsymbol{I}_N \otimes \boldsymbol{C}) & \boldsymbol{0} & \boldsymbol{0} \\ * & * & \boldsymbol{0} \\ * & * & -\gamma^2\boldsymbol{I}_N \end{bmatrix} \mathbb{E}\begin{bmatrix} \boldsymbol{X}(k) \\ \boldsymbol{X}(k-1) \\ \boldsymbol{W}(k) \end{bmatrix}. \end{aligned} \tag{31}$$

By summing (30) and (31), for any non-zero $\boldsymbol{\Gamma}(k) = \mathbb{E}\{\begin{bmatrix}\boldsymbol{X}^T(k) & \boldsymbol{X}^T(k-1) & \boldsymbol{W}^T(k)\end{bmatrix}^T\}$, condition (29) is satisfied when (32) (which is shown on the bottom of the next page) holds.

Inequality (32) is a bilinear matrix inequality (BMI) problem which has the properties of nonlinear programming and provides non-convex feasible solution. This kind of problem is difficult to solve computationally due to the lack of existance of off-the-shelf algorithms [59]. Therefore, to overcome this problem, (32) is converted into an LMI form as in [60]. To this aim (32) is first re-written by matrix factorization method as (33) (as shown on the bottom of the next page).

$$\begin{aligned}G(z) = {T_s}^3 z[\boldsymbol{I}_n \cdot (\tau z^4 + (T_s - 3\tau)z^3 + (3\tau - 2T_s)z^2 + (T_s - \tau)z) + (\mathcal{L}+\mathcal{P})((K_a - K_v T_s + K_s {T_s}^2)T_s r \\ + ((K_a - K_v T_s + K_s {T_s}^2)(1-r) - (2K_a - K_v T_s)r)T_s z + ((K_v T_s - 2K_a)(1-r) + K_a r)T_s z^2 + K_a T_s(1-r)z^3)]^{-1}.\end{aligned} \tag{26}$$

$$\begin{aligned}\mathbb{E}\{\Delta V(k)\} &= \mathbb{E}\begin{bmatrix}\boldsymbol{X}^T(k) & \boldsymbol{X}^T(k-1) & \boldsymbol{W}^T(k)\end{bmatrix} \\ &\quad \times \begin{bmatrix} \bar{\boldsymbol{A}}_d^T\boldsymbol{P}\bar{\boldsymbol{A}}_d + \boldsymbol{Q} - \boldsymbol{P} & \bar{\boldsymbol{A}}_d^T\boldsymbol{P}(\tilde{\boldsymbol{L}}r \otimes \boldsymbol{B}_d\boldsymbol{K}) & \bar{\boldsymbol{A}}_d^T\boldsymbol{P}(\boldsymbol{I}_N \otimes \boldsymbol{B}_d) \\ * & (\tilde{\boldsymbol{L}}r \otimes \boldsymbol{B}_d\boldsymbol{K})^T\boldsymbol{P}(\tilde{\boldsymbol{L}}r \otimes \boldsymbol{B}_d\boldsymbol{K}) - \boldsymbol{Q} & (\tilde{\boldsymbol{L}}r \otimes \boldsymbol{B}_d\boldsymbol{K})^T\boldsymbol{P}(\boldsymbol{I}_N \otimes \boldsymbol{B}_d) \\ * & * & (\boldsymbol{I}_N \otimes \boldsymbol{B}_d)^T\boldsymbol{P}(\boldsymbol{I}_N \otimes \boldsymbol{B}_d) \end{bmatrix} \mathbb{E}\begin{bmatrix} \boldsymbol{X}(k) \\ \boldsymbol{X}(k-1) \\ \boldsymbol{W}(k) \end{bmatrix}. \end{aligned} \tag{30}$$

Using Schur complement [59]–[61] to (33) yields,

$$\begin{bmatrix} \boldsymbol{Q}-\boldsymbol{P} & * & * & * & * \\ \mathbf{0} & -\boldsymbol{Q} & * & * & * \\ \mathbf{0} & \mathbf{0} & -\gamma^2\boldsymbol{I}_N & * & * \\ \bar{\boldsymbol{A}}_d & \tilde{\boldsymbol{L}}r\otimes\boldsymbol{B}_d\boldsymbol{K} & \boldsymbol{I}_N\otimes\boldsymbol{B}_d & -\boldsymbol{P}^{-1} & * \\ \boldsymbol{I}_N\otimes\boldsymbol{C} & \mathbf{0} & \mathbf{0} & \mathbf{0} & -\boldsymbol{I}_N \end{bmatrix} < \mathbf{0}. \tag{34}$$

Now, using change of variable technique for representing the controller gain $\boldsymbol{K}$ with a new variable $\boldsymbol{Z}$, as $\boldsymbol{K} = \boldsymbol{Z}\boldsymbol{P}_0$ as reported in [59], [60], [62], both sides of (34) are multiplied by $diag\{\boldsymbol{P}^{-1}, \boldsymbol{P}^{-1}, \boldsymbol{I}_N, \boldsymbol{I}_N, \boldsymbol{I}_N\}$. Now, by defining $\boldsymbol{P}^{-1} = \boldsymbol{I}_N \otimes \boldsymbol{P}_0{}^{-1}$, $\boldsymbol{Q} = \boldsymbol{I}_N \otimes \boldsymbol{Q}_0$ and $\boldsymbol{K} = \boldsymbol{Z}\boldsymbol{P}_0$, the LMI (14) is obtained. It is seen that (34) is an LMI with nonconvex constraints $\{\boldsymbol{P}^{-1}, \boldsymbol{Q}^{-1}\}$. Therefore, to overcome this problem, the following variables are introduced in (34):

$$\boldsymbol{P}^{-1}\boldsymbol{Q}\boldsymbol{P}^{-1} = \boldsymbol{M}, \boldsymbol{P}^{-1} = \bar{\boldsymbol{P}}, \text{and } \boldsymbol{Q}^{-1} = \bar{\boldsymbol{Q}}. \tag{35}$$

Equation (35) can be written into the LMI form (15), thus completing the proof.

C. Proof of Theorem 2

For LMIs (14) and (15), the matrices $\{\bar{\boldsymbol{P}}, \bar{\boldsymbol{Q}}, \boldsymbol{M}, \boldsymbol{I}_N\otimes\boldsymbol{A}_d, \boldsymbol{I}_N\otimes\boldsymbol{B}_d, \boldsymbol{I}_N\otimes\boldsymbol{C}, \gamma^2\boldsymbol{I}_N\}$ are block diagonal matrices and $\tilde{\boldsymbol{L}}$ is a symmetric matrix. Therefore, an orthogonal matrix $\boldsymbol{\Psi} \in \mathbb{R}^{N\times N}$ satisfying $\boldsymbol{\Psi}^T = \boldsymbol{\Psi}^{-1}$ such that $\boldsymbol{\Psi}^{-1}\tilde{\boldsymbol{L}}\boldsymbol{\Psi} = \boldsymbol{D}$ must exist, where $\boldsymbol{D}$ is a diagonal and real matrix where the entry of the diagonal are the eigenvalues of $\tilde{\boldsymbol{L}} = (\mathcal{L}+\mathcal{P})$, i.e., $\boldsymbol{D} = diag\{\lambda_1, \lambda_2, \ldots, \lambda_N\}$, with $\lambda_i = \lambda_i(\mathcal{L}+\mathcal{P})$, $i = 1, 2, \ldots, N$.

By defining $\bar{\boldsymbol{\Psi}} = diag\{\bar{\boldsymbol{\Psi}}_0, \bar{\boldsymbol{\Psi}}_0, \bar{\boldsymbol{\Psi}}_0, \bar{\boldsymbol{\Psi}}_0, \bar{\boldsymbol{\Psi}}_0\}$ and $\bar{\boldsymbol{\Psi}}^{-1} = diag\{\bar{\boldsymbol{\Psi}}_0^{-1}, \bar{\boldsymbol{\Psi}}_0^{-1}, \bar{\boldsymbol{\Psi}}_0^{-1}, \bar{\boldsymbol{\Psi}}_0^{-1}, \bar{\boldsymbol{\Psi}}_0^{-1}\}$ with $\bar{\boldsymbol{\Psi}}_0 = \boldsymbol{\Psi}\otimes\boldsymbol{I}_3$, we define the matrices $\tilde{\boldsymbol{\Xi}}_1$ as in (36) (which is shown on the bottom of the page) and $\tilde{\boldsymbol{\Xi}}_2$ as:

$$\tilde{\boldsymbol{\Xi}}_2 = \bar{\boldsymbol{\Psi}}^{-1}\boldsymbol{\Xi}_2\bar{\boldsymbol{\Psi}}^{-1} = \begin{bmatrix} -\bar{\boldsymbol{\Psi}}_0^{-1}\boldsymbol{M}\bar{\boldsymbol{\Psi}}_0 & \bar{\boldsymbol{\Psi}}_0^{-1}\bar{\boldsymbol{P}}\bar{\boldsymbol{\Psi}}_0 \\ * & -\bar{\boldsymbol{\Psi}}_0^{-1}\bar{\boldsymbol{Q}}\bar{\boldsymbol{\Psi}}_0 \end{bmatrix} < \mathbf{0}. \tag{37}$$

By using the properties of the Kronecker product (i.e., Equations 2 and 3 of [34]) in (36) and (37), the matrix $\tilde{\boldsymbol{\Xi}}_1$ can be recast as in (38) (which is shown on the bottom of the page) while $\tilde{\boldsymbol{\Xi}}_2$ can be written as:

$$\tilde{\boldsymbol{\Xi}}_2 = \begin{bmatrix} -\boldsymbol{I}_N\otimes\boldsymbol{M}_0 & \boldsymbol{I}_N\otimes\bar{\boldsymbol{P}}_0 \\ * & -\boldsymbol{I}_N\otimes\bar{\boldsymbol{Q}}_0 \end{bmatrix} < \mathbf{0}. \tag{39}$$

Since $\boldsymbol{\Psi}$ is an orthogonal matrix, thus satisfying $\boldsymbol{\Psi}^T = \boldsymbol{\Psi}^{-1}$, the following holds:

$$\boldsymbol{\Xi}_1 \Leftrightarrow \tilde{\boldsymbol{\Xi}}_1 < \mathbf{0}, \boldsymbol{\Xi}_2 \Leftrightarrow \tilde{\boldsymbol{\Xi}}_2 < \mathbf{0}. \tag{40}$$

Furthermore, all the submatrices in LMIs (38) and (39) are block diagonal. Hence, (38) and (39) can be re-written by using the decomposed form in (16) and (17), thus completing the proof of Theorem 2.

D. Proof of Theorem 3

By using the spectral composition of the matrix $\tilde{\boldsymbol{L}} = (\mathcal{L}+\mathcal{P})$ introduced in Appendix C (i.e., $\boldsymbol{\Psi}^{-1}\tilde{\boldsymbol{L}}\boldsymbol{\Psi} = \boldsymbol{D}$), the transfer function of the closed-loop system (26) can be

$$\begin{bmatrix} \bar{\boldsymbol{A}}_d^T\boldsymbol{P}\bar{\boldsymbol{A}}_d + \boldsymbol{Q} - \boldsymbol{P} + (\boldsymbol{I}_N\otimes\boldsymbol{C})^T(\boldsymbol{I}_N\otimes\boldsymbol{C}) & \bar{\boldsymbol{A}}_d^T\boldsymbol{P}(\tilde{\boldsymbol{L}}r\otimes\boldsymbol{B}_d\boldsymbol{K}) & \bar{\boldsymbol{A}}_d^T\boldsymbol{P}(\boldsymbol{I}_N\otimes\boldsymbol{B}_d) \\ * & (\tilde{\boldsymbol{L}}r\otimes\boldsymbol{B}_d\boldsymbol{K})^T\boldsymbol{P}(\tilde{\boldsymbol{L}}r\otimes\boldsymbol{B}_d\boldsymbol{K}) - \boldsymbol{Q} & (\tilde{\boldsymbol{L}}r\otimes\boldsymbol{B}_d\boldsymbol{K})^T\boldsymbol{P}(\boldsymbol{I}_N\otimes\boldsymbol{B}_d) \\ * & * & (\boldsymbol{I}_N\otimes\boldsymbol{B}_d)^T\boldsymbol{P}(\boldsymbol{I}_N\otimes\boldsymbol{B}_d) - \gamma^2\boldsymbol{I}_N \end{bmatrix} < \mathbf{0}. \tag{32}$$

$$\begin{bmatrix} \boldsymbol{Q}-\boldsymbol{P} & \mathbf{0} & \mathbf{0} \\ * & -\boldsymbol{Q} & \mathbf{0} \\ * & * & -\gamma^2\boldsymbol{I}_N \end{bmatrix} + \begin{bmatrix} (\boldsymbol{I}_N\otimes\boldsymbol{C})^T \\ \mathbf{0} \\ \mathbf{0} \end{bmatrix} \begin{bmatrix} (\boldsymbol{I}_N\otimes\boldsymbol{C}) & \mathbf{0} & \mathbf{0} \end{bmatrix} + \begin{bmatrix} \bar{\boldsymbol{A}}_d^T \\ (\tilde{\boldsymbol{L}}r\otimes\boldsymbol{B}_d\boldsymbol{K})^T \\ (\boldsymbol{I}_N\otimes\boldsymbol{B}_d)^T \end{bmatrix} \boldsymbol{P} \begin{bmatrix} \bar{\boldsymbol{A}}_d & (\tilde{\boldsymbol{L}}r\otimes\boldsymbol{B}_d\boldsymbol{K}) & (\boldsymbol{I}_N\otimes\boldsymbol{B}_d) \end{bmatrix} < \mathbf{0}. \tag{33}$$

$$\tilde{\boldsymbol{\Xi}}_1 = \bar{\boldsymbol{\Psi}}^{-1}\boldsymbol{\Xi}_1\bar{\boldsymbol{\Psi}}^{-1} = \begin{bmatrix} \bar{\boldsymbol{\Psi}}_0^{-1}(\boldsymbol{M}-\bar{\boldsymbol{P}})\bar{\boldsymbol{\Psi}}_0 & * & * & * & * \\ \mathbf{0} & -\bar{\boldsymbol{\Psi}}_0^{-1}\boldsymbol{M}\bar{\boldsymbol{\Psi}}_0 & * & * & * \\ \mathbf{0} & \mathbf{0} & -\bar{\boldsymbol{\Psi}}_0^{-1}(\gamma^2\boldsymbol{I}_N)\bar{\boldsymbol{\Psi}}_0 & * & * \\ \bar{\boldsymbol{\Psi}}_0^{-1}((\boldsymbol{I}_N\otimes\boldsymbol{A}_d)\bar{\boldsymbol{P}} + \tilde{\boldsymbol{L}}(1-r)\otimes\boldsymbol{B}_d\boldsymbol{Z})\bar{\boldsymbol{\Psi}}_0 & \bar{\boldsymbol{\Psi}}_0^{-1}(\tilde{\boldsymbol{L}}r\otimes\boldsymbol{B}_d\boldsymbol{Z})\bar{\boldsymbol{\Psi}}_0 & \bar{\boldsymbol{\Psi}}_0^{-1}(\boldsymbol{I}_N\otimes\boldsymbol{B}_d)\bar{\boldsymbol{\Psi}}_0 & -\bar{\boldsymbol{\Psi}}_0^{-1}\bar{\boldsymbol{P}}\bar{\boldsymbol{\Psi}}_0 & * \\ \bar{\boldsymbol{\Psi}}_0^{-1}((\boldsymbol{I}_N\otimes\boldsymbol{C})\bar{\boldsymbol{P}})\bar{\boldsymbol{\Psi}}_0 & \mathbf{0} & \mathbf{0} & \mathbf{0} & -\bar{\boldsymbol{\Psi}}_0^{-1}\boldsymbol{I}_N\bar{\boldsymbol{\Psi}}_0 \end{bmatrix} < \mathbf{0}. \tag{36}$$

$$\tilde{\boldsymbol{\Xi}}_1 = \begin{bmatrix} \boldsymbol{I}_N\otimes\boldsymbol{M}_0 - \boldsymbol{I}_N\otimes\bar{\boldsymbol{P}}_0 & * & * & * & * \\ \mathbf{0} & -\boldsymbol{I}_N\otimes\boldsymbol{M}_0 & * & * & * \\ \mathbf{0} & \mathbf{0} & -\gamma^2\boldsymbol{I}_N & * & * \\ ((\boldsymbol{I}_N\otimes\boldsymbol{A}_d)(\boldsymbol{I}_N\otimes\bar{\boldsymbol{P}}_0) + \boldsymbol{D}(1-r)\otimes\boldsymbol{B}_d\boldsymbol{Z}) & \boldsymbol{D}r\otimes\boldsymbol{B}_d\boldsymbol{Z} & \boldsymbol{I}_N\otimes\boldsymbol{B}_d & -\boldsymbol{I}_N\otimes\bar{\boldsymbol{P}}_0 & * \\ (\boldsymbol{I}_N\otimes\boldsymbol{C})(\boldsymbol{I}_N\otimes\bar{\boldsymbol{P}}_0) & \mathbf{0} & \mathbf{0} & \mathbf{0} & -\boldsymbol{I}_N \end{bmatrix} < \mathbf{0}. \tag{38}$$

$$\begin{aligned} G(z) &= {T_s}^3 z[\boldsymbol{I}_n \cdot (\tau z^4 + (T_s - 3\tau)z^3 + (3\tau - 2T_s)z^2 + (T_s - \tau)z) + \boldsymbol{\Psi D \Psi}^{-1}((K_a - K_v T_s + K_s {T_s}^2)T_s r \\ &\quad + ((K_a - K_v T_s + K_s {T_s}^2)(1-r) - (2K_a - K_v T_s)r)T_s z + ((K_v T_s - 2K_a)(1-r) + K_a r)T_s z^2 + K_a T_s (1-r)z^3)]^{-1} \\ &= \boldsymbol{\Psi}[{T_s}^3 z[\boldsymbol{I}_n \cdot (\tau z^4 + (T_s - 3\tau)z^3 + (3\tau - 2T_s)z^2 + (T_s - \tau)z) + \boldsymbol{D}((K_a - K_v T_s + K_s {T_s}^2)T_s r \\ &\quad + ((K_a - K_v T_s + K_s {T_s}^2)(1-r) - (2K_a - K_v T_s)r)T_s z + ((K_v T_s - 2K_a)(1-r) + K_a r)T_s z^2 + K_a T_s (1-r)z^3)]^{-1}]\boldsymbol{\Psi}^{-1}. \end{aligned} \tag{41}$$

$$\begin{aligned} G_i(z) &= {T_s}^3 z[(\tau z^4 + (T_s - 3\tau)z^3 + (3\tau - 2T_s)z^2 + (T_s - \tau)z) + \lambda_i((K_a - K_v T_s + K_s {T_s}^2)T_s r \\ &\quad + ((K_a - K_v T_s + K_s {T_s}^2)(1-r) - (2K_a - K_v T_s)r)T_s z + ((K_v T_s - 2K_a)(1-r) + K_a r)T_s z^2 + K_a T_s (1-r)z^3)]^{-1}. \end{aligned} \tag{43}$$

$$\begin{aligned} &\| G_i(z) \|_{H_\infty} \\ &= \sup_\omega \sqrt{\begin{array}{c} ({T_s}^6(\cos^2(\omega T_s) + \sin^2(\omega T_s)))/[(\tau(\cos^4(\omega T_s) + \sin^4(\omega T_s) - 6\cos^2(\omega T_s)\sin^2(\omega T_s)) + \\ \lambda_i(T_s - 3\tau + K_a T_s(1-r))(\cos^3(\omega T_s) - 3\cos(\omega T_s)\sin^2(\omega T_s)) + \\ \lambda_i(3\tau + ((K_v T_s - 2K_a)(1-r) + K_a r - 2)T_s)(\cos(\omega T_s) - \sin^2(\omega T_s)) + \\ \lambda_i(((K_a - K_v T_s + K_s {T_s}^2)(1-r) - (2K_a - K_v T_s)r + 1)T_s - \tau)\cos(\omega T_s) + \lambda_i(K_a - K_v T_s + K_s {T_s}^2)T_s r)^2 \\ +(\tau(4\cos^3(\omega T_s)\sin(\omega T_s) - 4\cos(\omega T_s)\sin^3(\omega T_s)) + \lambda_i(T_s - 3\tau + K_a T_s(1-r))(3\cos^2(\omega T_s)\sin(\omega T_s) - \sin^3(\omega T_s)) \\ +\lambda_i(3\tau + ((K_v T_s - 2K_a)(1-r) + K_a r - 2)T_s)(2\cos(\omega T_s)\sin(\omega T_s)) + \\ \lambda_i(((K_a - K_v T_s + K_s {T_s}^2)(1-r) - (2K_a - K_v T_s)r + 1)T_s - \tau)\sin(\omega T_s))^2] \end{array}} \\ &\geq \frac{1}{\lambda_i K_s} \geq \frac{1}{\lambda_{min} K_s}, \forall i = 1, 2, \ldots, N. \end{aligned} \tag{45}$$

re-written as (41) (which are shown on the top of the page), which implies,

$$G(z) = \boldsymbol{\Psi} \begin{bmatrix} G_1(z) & & & \\ & G_2(z) & & \\ & & \ddots & \\ & & & G_N(z) \end{bmatrix} \boldsymbol{\Psi}^{-1}, \tag{42}$$

with $G_i(z)$ being given in (43) (which is shown on the top of the page) where $\lambda_i = \lambda_i(\mathcal{L} + \mathcal{P})$, $i = 1, 2, \ldots, N$.

Consequently, the γ-gain in (19) can be obtained as:

$$\begin{aligned} \gamma &= \| G(z) \|_{H_\infty} = \sup_\omega [\sigma_{max}(G(e^{j\omega T_s}))] \\ &= \sup_\omega \sqrt{\lambda(\bar{G}(e^{j\omega T_s})G(e^{j\omega T_s}))} \\ &= \sup_\omega \max_i \sqrt{\bar{G}_i(e^{j\omega T_s})G_i(e^{j\omega T_s})} \\ &= \max_i \| G_i(z) \|_{H_\infty}, \quad \forall i = 1, 2, \ldots, N. \end{aligned} \tag{44}$$

where, $\bar{G}(\cdot)$ represents the complex conjugate of $G(\cdot)$. By replacing z with $e^{j\omega T_s} = \cos(\omega T_s) + j\sin(\omega T_s)$ in (44), $\| G_i(z) \|_{H_\infty}$ can be lower bounded as (45) (which is shown on the top of the page).

Hence, $\gamma \geq \dfrac{1}{\lambda_{min} K_s}$ holds.

E. Proof of Corollaries 1, 2 and 3

If θ is a positive real number for which $\lambda_{min}(\mathcal{L} + \mathcal{P}) \leq \theta$, then from Theorem 3

$$\gamma \geq \frac{1}{\lambda_{min}(\mathcal{L} + \mathcal{P})K_s} \geq \frac{1}{\theta K_s}. \tag{46}$$

In [15], it was proven that

$$\lambda_{min}(\mathcal{L} + \mathcal{P}) \leq \frac{\Omega(N)}{N}, \tag{47}$$

while in Lemma 3 and Lemma 4 in [4] proved that

$$\lambda_{min}(\mathcal{L}_{BPF} + \mathcal{P}_{BPF}) \leq \frac{\pi^2}{N^2}, \tag{48}$$

$$\lambda_{min}(\mathcal{L}_{BPLF} + \mathcal{P}_{BPLF}) \leq 1 + \frac{\pi^2}{N^2}. \tag{49}$$

By using (46) with either (47), (48) or (49), Corollaries 1, 2 and 3, hold, respectively.

REFERENCES

[1] U. Montanaro *et al.*, "Towards connected autonomous driving: Review of use-cases," *Vehicle Syst. Dyn.*, vol. 57, no. 6, pp. 779–814, Jun. 2019.

[2] J. K. Hedrick, M. Tomizuka, and P. Varaiya, "Control issues in automated highway systems," *IEEE Control Syst.*, vol. 14, no. 6, pp. 21–32, Dec. 1994.

[3] G. J. L. Naus, R. P. A. Vugts, J. Ploeg, M. J. G. van de Molengraft, and M. Steinbuch, "String-stable CACC design and experimental validation: A frequency-domain approach," *IEEE Trans. Veh. Technol.*, vol. 59, no. 9, pp. 4268–4279, Nov. 2010.

[4] Y. Zheng, S. E. Li, J. Wang, L. Y. Wang, and K. Li, "Stability and scalability of homogeneous vehicular platoon: Study on the influence of information flow topologies," *IEEE Trans. Intell. Transp. Syst.*, vol. 17, no. 1, pp. 14–26, Jan. 2016.

[5] S. E. Li, Y. Zheng, K. Li, and J. Wang, "An overview of vehicular platoon control under the four-component framework," in *Proc. IEEE Intell. Vehicles Symp. (IV)*, Jun. 2015, pp. 286–291.

[6] D. Jia and D. Ngoduy, "Enhanced cooperative car-following traffic model with the combination of V2 V and V2I communication," *Transp. Res. B, Methodol.*, vol. 90, pp. 172–191, Aug. 2016.

[7] S. Darbha and P. R. Pagilla, "Limitations of employing undirected information flow graphs for the maintenance of rigid formations for heterogeneous vehicles," *Int. J. Eng. Sci.*, vol. 48, no. 11, pp. 1164–1178, Nov. 2010.

[8] S. E. Li, X. Qin, Y. Zheng, J. Wang, K. Li, and H. Zhang, "Distributed platoon control under topologies with complex eigenvalues: Stability analysis and controller synthesis," *IEEE Trans. Control Syst. Technol.*, vol. 27, no. 1, pp. 206–220, Jan. 2019.

[9] U. Montanaro, S. Fallah, M. Dianati, D. Oxtoby, T. Mizutani, and A. Mouzakitis, "On a fully self-organizing vehicle platooning supported by cloud computing," in *Proc. 5th Int. Conf. Internet Things, Syst., Manage. Secur.*, Oct. 2018, pp. 295–302.

[10] Y. Zheng, S. E. Li, K. Li, and L.-Y. Wang, "Stability margin improvement of vehicular platoon considering undirected topology and asymmetric control," *IEEE Trans. Control Syst. Technol.*, vol. 24, no. 4, pp. 1253–1265, Jul. 2016.

[11] L. Xu, L. Y. Wang, G. Yin, and H. Zhang, "Impact of communication erasure channels on the safety of highway vehicle platoons," *IEEE Trans. Intell. Transp. Syst.*, vol. 16, no. 3, pp. 1456–1468, Jun. 2015.

[12] C. Lei, E. M. van Eenennaam, W. Klein Wolterink, J. Ploeg, G. Karagiannis, and G. Heijenk, "Evaluation of CACC string stability using SUMO, simulink, and OMNeT++," *EURASIP J. Wireless Commun. Netw.*, vol. 2012, no. 1, p. 116, Dec. 2012.

[13] K. K. Lee and S. T. Chanson, "Packet loss probability for real-time wireless communications," *IEEE Trans. Veh. Technol.*, vol. 51, no. 6, pp. 1569–1575, Nov. 2002.

[14] U. Montanaro, M. Tufo, G. Fiengo, M. di Bernardo, A. Salvi, and S. Santini, "Extended cooperative adaptive cruise control," in *Proc. IEEE Intell. Vehicles Symp. Proc.*, Jun. 2014, pp. 605–610.

[15] Y. Zheng, S. E. Li, K. Li, and W. Ren, "Platooning of connected vehicles with undirected topologies: Robustness analysis and distributed H-infinity controller synthesis," *IEEE Trans. Intell. Transp. Syst.*, vol. 19, no. 5, pp. 1353–1364, May 2018.

[16] Y. Zheng, S. E. Li, K. Li, F. Borrelli, and J. K. Hedrick, "Distributed model predictive control for heterogeneous vehicle platoons under unidirectional topologies," *IEEE Trans. Control Syst. Technol.*, vol. 25, no. 3, pp. 899–910, May 2017.

[17] S. Wen and G. Guo, "Cooperative control and communication of connected vehicles considering packet dropping rate," *Int. J. Syst. Sci.*, vol. 49, no. 13, pp. 2808–2825, Oct. 2018.

[18] F. Gao, Y. Zheng, S. E. Li, and D. Kum, "Robust control of heterogeneous vehicular platoon with uncertain dynamics and communication delay," *IET Intell. Transp. Syst.*, vol. 10, no. 7, pp. 503–513, Sep. 2016.

[19] S. E. Li *et al.*, "Dynamical modeling and distributed control of connected and automated vehicles: Challenges and opportunities," *IEEE Intell. Transp. Syst. Mag.*, vol. 9, no. 3, pp. 46–58, May 2017.

[20] J.-W. Kwon and D. Chwa, "Adaptive bidirectional platoon control using a coupled sliding mode control method," *IEEE Trans. Intell. Transp. Syst.*, vol. 15, no. 5, pp. 2040–2048, Oct. 2014.

[21] L. Xu, W. Zhuang, G. Yin, and C. Bian, "Stable longitudinal control of heterogeneous vehicular platoon with disturbances and information delays," *IEEE Access*, vol. 6, pp. 69794–69806, 2018.

[22] Y. Tang, M. Yan, P. Yang, and L. Zuo, "Consensus based control algorithm for vehicle platoon with packet losses," in *Proc. 37th Chin. Control Conf. (CCC)*, Jul. 2018, pp. 7684–7689.

[23] J. Ploeg, D. P. Shukla, N. van de Wouw, and H. Nijmeijer, "Controller synthesis for string stability of vehicle platoons," *IEEE Trans. Intell. Transp. Syst.*, vol. 15, no. 2, pp. 854–865, Apr. 2014.

[24] M. di Bernardo, A. Salvi, and S. Santini, "Distributed consensus strategy for platooning of vehicles in the presence of time-varying heterogeneous communication delays," *IEEE Trans. Intell. Transp. Syst.*, vol. 16, no. 1, pp. 102–112, Feb. 2015.

[25] D. Swaroop, J. K. Hedrick, and S. B. Choi, "Direct adaptive longitudinal control of vehicle platoons," *IEEE Trans. Veh. Technol.*, vol. 50, no. 1, pp. 150–161, Jan. 2001.

[26] H. Zhou, R. Saigal, F. Dion, and L. Yang, "Vehicle platoon control in high-latency wireless communications environment: Model predictive control method," *Transp. Res. Rec., J. Transp. Res. Board*, vol. 2324, no. 1, pp. 81–90, Jan. 2012.

[27] C. Lei, E. M. van Eenennaam, W. K. Wolterink, G. Karagiannis, G. Heijenk, and J. Ploeg, "Impact of packet loss on CACC string stability performance," in *Proc. 11th Int. Conf. ITS Telecommun.*, Aug. 2011, pp. 381–386.

[28] S. Oncu, J. Ploeg, N. van de Wouw, and H. Nijmeijer, "Cooperative adaptive cruise control: Network-aware analysis of string stability," *IEEE Trans. Intell. Transp. Syst.*, vol. 15, no. 4, pp. 1527–1537, Aug. 2014.

[29] L. Xu, W. Zhuang, G. Yin, C. Bian, and H. Wu, "Modeling and robust control of heterogeneous vehicle platoons on curved roads subject to disturbances and delays," *IEEE Trans. Veh. Technol.*, vol. 68, no. 12, pp. 11551–11564, Sep. 2019.

[30] K. Halder *et al.*, "Distributed controller design for vehicle platooning under packet drop scenario," in *Proc. 23rd IEEE Int. Conf. Intell. Transp. Syst.*, May 2020, pp. 1–4.

[31] C. Huang and X. Ye, "Cooperative output regulation of heterogeneous multi-agent systems: An H-infinity criterion," *IEEE Trans. Autom. Control*, vol. 59, no. 1, pp. 267–273, 2013.

[32] G. Ferrari-Trecate, L. Galbusera, M. P. E. Marciandi, and R. Scattolini, "Model predictive control schemes for consensus in multi-agent systems with single-and double-integrator dynamics," *IEEE Trans. Autom. Control*, vol. 54, no. 11, pp. 2560–2572, 2009.

[33] Z. Cheng, H.-T. Zhang, M.-C. Fan, and G. Chen, "Distributed consensus of multi-agent systems with input constraints: A model predictive control approach," *IEEE Trans. Circuits Syst. I, Reg. Papers*, vol. 62, no. 3, pp. 825–834, Mar. 2015.

[34] Y.-J. Pan, H. Werner, Z. Huang, and M. Bartels, "Distributed cooperative control of leader–follower multi-agent systems under packet dropouts for quadcopters," *Syst. Control Lett.*, vol. 106, pp. 47–57, Aug. 2017.

[35] H. Zhang, F. L. Lewis, and A. Das, "Optimal design for synchronization of cooperative systems: State feedback, observer and output feedback," *IEEE Trans. Autom. Control*, vol. 56, no. 8, pp. 1948–1952, Aug. 2011.

[36] Y. Liu and Y. Jia, "Robust H_∞ consensus control of uncertain multi-agent systems with time delays," *Int. J. Control, Autom. Syst.*, vol. 9, no. 6, pp. 1086–1094, Dec. 2011.

[37] F. Wang, G. Wen, Z. Peng, T. Huang, and Y. Yu, "Event-triggered consensus of general linear multiagent systems with data sampling and random packet losses," *IEEE Trans. Syst., Man, Cybern. Syst.*, early access, Feb. 26, 2019, doi: 10.1109/TSMC.2019.2896772.

[38] J. Wu and Y. Shi, "Average consensus in multi-agent systems with time-varying delays and packet losses," in *Proc. Amer. Control Conf. (ACC)*, Jun. 2012, pp. 1579–1584.

[39] W. Zhang, Y. Tang, T. Huang, and J. Kurths, "Sampled-data consensus of linear multi-agent systems with packet losses," *IEEE Trans. Neural Netw. Learn. Syst.*, vol. 28, no. 11, pp. 2516–2527, Nov. 2017.

[40] D. Jia and D. Ngoduy, "Platoon based cooperative driving model with consideration of realistic inter-vehicle communication," *Transp. Res. C, Emerg. Technol.*, vol. 68, pp. 245–264, Jul. 2016.

[41] K. Zhou *et al.*, *Robust and Optimal Control*, vol. 40. Upper Saddle River, NJ, USA: Prentice-Hall, 1996.

[42] J.-S. Song and X.-H. Chang, "H_∞ controller design of networked control systems with a new quantization structure," *Appl. Math. Comput.*, vol. 376, Jul. 2020, Art. no. 125070.

[43] X.-H. Chang, J. H. Park, and J. Zhou, "Robust static output feedback h-infinity control design for linear systems with polytopic uncertainties," *Syst. Control Lett.*, vol. 85, pp. 23–32, Aug. 2015.

[44] X.-H. Chang, Y. Liu, and M. Shen, "Resilient control design for lateral motion regulation of intelligent vehicle," *IEEE/ASME Trans. Mechatronics*, vol. 24, no. 6, pp. 2488–2497, Dec. 2019.

[45] C. Zhao, L. Cai, and P. Cheng, "Stability analysis of vehicle platooning with limited communication range and random packet losses," *IEEE Internet Things J.*, early access, Jun. 24, 2020, doi: 10.1109/JIOT.2020.3004573.

[46] S. E. Li, F. Gao, K. Li, L.-Y. Wang, K. You, and D. Cao, "Robust longitudinal control of multi-vehicle systems—A distributed h-infinity method," *IEEE Trans. Intell. Transp. Syst.*, vol. 19, no. 9, pp. 2779–2788, Aug. 2017.

[47] L. Xu, W. Zhuang, G. Yin, G. Li, and C. Bian, "Simultaneous longitudinal and lateral control of vehicle platoon subject to stochastic communication delays," *J. Dyn. Syst., Meas., Control*, vol. 141, no. 4, pp. 044503-1–044503-9, Apr. 2019.

[48] C. Godsil and G. F. Royle, *Algebraic Graph Theory*, vol. 207. New York, NY, USA: Springer, 2013.

[49] F. L. Lewis, H. Zhang, K. Hengster-Movric, and A. Das, *Cooperative Control of Multi-Agent Systems: Optimal and Adaptive Design Approaches*. London, U.K.: Springer, 2013.

[50] K. Ogata *et al.*, *Discrete-Time Control System*, vol. 2. Upper Saddle River, NJ, USA: Prentice-Hall, 1995.

[51] G. F. Franklin *et al.*, *Digital Control of Dynamic Systems*, vol. 3. Reading, MA, USA: Addison-Wesley, 1998.

[52] K. Halder, S. Das, and A. Gupta, "Transformation of LQR weights for discretization invariant performance of PI/PID dominant pole placement controllers," *Robotica*, vol. 38, no. 2, pp. 271–298, Feb. 2020.

[53] Z. Wang, F. Yang, D. W. Ho, and X. Liu, "Robust H-infinity control for networked systems with random packet losses," *IEEE Trans. Syst., Man, Cybern. B. Cybern.*, vol. 37, no. 4, pp. 916–924, Aug. 2007.

[54] K. Halder, D. Bose, and A. Gupta, "Stability and performance analysis of networked control systems: A lifted sample-time approach with L_2 induced norm," *ISA Trans.*, vol. 86, pp. 62–72, Mar. 2019.
[55] K. Halder, S. Das, S. Dasgupta, S. Banerjee, and A. Gupta, "Controller design for networked control systems—An approach based on l2 induced norm," *Nonlinear Anal., Hybrid Syst.*, vol. 19, pp. 134–145, 2016.
[56] J. Lofberg, "Yalmip: A toolbox for modeling and optimization in MATLAB," in *2004 IEEE Int. Conf. Robot. Autom.*, Apr. 2004, pp. 284–289.
[57] *YALMIP*. Accessed: Feb. 2018. [Online]. Available: https://yalmip.github.io/
[58] J. F. Sturm, "Using SeDuMi 1.02, a MATLAB toolbox for optimization over symmetric cones," *Optim. Methods Softw.*, vol. 11, nos. 1–4, pp. 625–653, Jan. 1999.
[59] J. G. VanAntwerp and R. D. Braatz, "A tutorial on linear and bilinear matrix inequalities," *J. Process Control*, vol. 10, no. 4, pp. 363–385, Aug. 2000.
[60] S. Boyd, L. El Ghaoui, E. Feron, and V. Balakrishnan, *Linear Matrix Inequalities System Control Theory*. Philadelphia, PA, USA: SIAM, 1994.
[61] D. Carlson, "What are schur complements, anyway?" *Linear Algebra its Appl.*, vol. 74, pp. 257–275, Feb. 1986.
[62] M. V. Kothare, V. Balakrishnan, and M. Morari, "Robust constrained model predictive control using linear matrix inequalities," *Automatica*, vol. 32, no. 10, pp. 1361–1379, Oct. 1996.

Kaushik Halder received the B.Tech. degree in electronics and instrumentation engineering from the Haldia Institute of Technology, Haldia, India, in 2008, and the M.E. degree in power engineering and the Ph.D. degree in engineering from Jadavpur University, Kolkata, India, in 2010 and 2018, respectively. He was an Assistant Professor in Electronics and Instrumentation Engineering with the National Institute of Science and Technology, Brahmapur, India, from 2010 to 2013. He is currently a Post-Doctoral Research Fellow with the Department of Mechanical Engineering Sciences, University of Surrey, Guildford, U.K. He has authored or coauthored more than 20 research articles in refereed scientific journals and conferences. His research interests include control theory, networked control systems, and vehicle platooning.

Umberto Montanaro received the "Laurea" (M.Sc.) degree in computer science engineering *(cum laude)* from the University of Naples Federico II, Naples, Italy, in 2005, and the Ph.D. degree in control engineering and the second Ph.D. degree in mechanical engineering from the University of Naples Federico II, in 2009 and 2016, respectively. From 2010 to 2013, he was a Research Fellow with the Italian National Research Council (Istituto Motori), and he served as a temporary Lecturer in Automation and Process Control at the University of Naples Federico II. He is currently a Lecturer in Autonomous Systems and Control Engineering with the Department of Mechanical Engineering Sciences, University of Surrey, Guildford, U.K. The scientific results he has obtained up to now have been the subject of more than 60 scientific articles published in peer-reviewed international scientific journals and conferences. His research interests include control theory to control application and include adaptive control, enhanced model reference adaptive control (EMRAC), control of piecewise affine systems, control of mechatronics systems, automotive systems, control of networked systems, connected autonomous vehicles, and vehicle platooning.

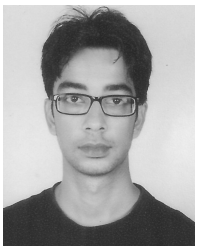

Shilp Dixit received the M.Sc. degree (Hons.) in automotive technology from the Eindhoven University of Technology, Eindhoven, The Netherlands, in 2015, and the Ph.D. degree in automotive engineering from the University of Surrey, U.K., in 2019. From 2010 to 2012, he worked in the field of Technology Consulting at Deloitte Consulting LLP, before making the switch to vehicle dynamics and control in 2012. Since has also worked as a Researcher at Tata Motors Ltd., and Flanders Make. His research interests include the control of mechatronics systems, vehicle dynamics and control, trajectory planning and tracking for autonomous vehicles, and intelligent vehicles.

Mehrdad Dianati (Senior Member, IEEE) was a Professor with the 5G Innovation Centre (5GIC), University of Surrey, where he is currently a Visiting Professor. He is also a Professor of Autonomous and Connected Vehicles with the Warwick Manufacturing Group (WMG), University of Warwick, U.K. He has been involved in a number of national and international projects as the project leader and work-package leader in recent years. He has worked in the industry for more than nine years, as a Senior Software/Hardware Developer and the Director of Research and Development. Frequently, he had provided voluntary services to the research community in various editorial roles; for example, he has served as an Associate Editor for the IEEE TRANSACTIONS ON VEHICULAR TECHNOLOGY, *IET Communications*, and journal of *Wireless Communications and Mobile Computing* (Wiley).

Alexandros Mouzakitis is currently the Head of the Electrical, Electronics and Software Engineering Research Department, Jaguar Land Rover. He has over 15 years of technological and managerial experience, especially in the area of automotive embedded systems. His current role is responsible for leading a multidisciplinary research and technology department dedicated to deliver a portfolio of advanced research projects in the areas of human-machine interface, digital transformation, self-learning vehicle, smart/connected systems, and onboard/off board data platforms. In previous position at JLR, he served as the Head of the Model-based Product Engineering Department, responsible for model-based development and automated testing standards and processes.

Saber Fallah is currently an Associate Professor with the University of Surrey, where he is also the Director of the Connected and Autonomous Vehicles Lab (CAV-Lab), Department of Mechanical Engineering Sciences. Since joining the University of Surrey, he has contributed to securing research funding from EPSRC, Innovate UK, EU, KTP, and industry. His work has contributed to the state-of-the-art research in the areas of connected autonomous vehicles and advanced driver assistance systems. So far, his research has produced four patents and more than 40 peer-reviewed publications in high-quality journals and well-known conferences. He is also coauthor of a textbook titled *Electric and Hybrid Vehicles: Technologies, Modeling and Control—A Mechatronic Approach* (John Wiley, 2014). The book addresses the fundamentals of mechatronic design in hybrid and electric vehicles.

Dr. Fallah is the co-editor of the book of conference proceedings resulted from the organization of the TAROS 2017 conference published by Springer in 2017.